

EVALUATION OF HEAVY TRUCK ROLLOVER ACCIDENTS

Jeffrey L. Evans
Stephen A. Batzer
Stanley B. Andrews
Renfroe Engineering, Inc.
United States
Paper Number 05-0140

ABSTRACT

Given the large size and weight of heavy trucks, also known as tractor-trailer vehicles, a serious safety threat can be posed to the vehicle's occupants in the event of a rollover collision. This study evaluated heavy vehicle accidents from 1994-2002 by submitting queries to the Fatality Analysis Reporting System (FARS), which is administered by the National Highway Traffic Safety Administration (NHTSA), in order to determine the number of incapacitating and fatal injuries that occurred when the occupants were contained in the cab during a rollover accident. The specific query was for rollover accidents of heavy trucks where the rollover was the most harmful event; the rollover was either the first or subsequent event; the truck received severe and disabling deformation; the occupants were not ejected; and the injuries sustained were either incapacitating or fatal. This rollover accident data was also compared with the total number of heavy truck accidents where incapacitating or fatal injuries occurred as reported by FARS for the 1994-2002 time period. The average percent of persons involved in accidents that matched the rollover query was 18%, with a high of 21% in 2002 and a low of 17% occurring in 1994, 1995, and 1997. The average percentage per year of incapacitating and fatal injuries for restrained occupants during this time period was determined by further analyzing the data obtained from the above stated rollover query and was found to be 35%. The conclusion drawn from this study is that significant injuries can occur from rollover accidents of heavy trucks even for restrained occupants. Rollover crashworthiness of heavy trucks is also evaluated in this paper.

INTRODUCTION

Heavy trucks (those having a gross vehicle weight rating greater than 10,000 pounds) are an essential part of the transport of a vast array of commercial, industrial, and consumer products in the United States. According to the National Center for Statistics and Analysis, a division of NHTSA, in 2001 7,857,674 heavy trucks were registered in the

United States, accounting for 4% of all registered vehicles. In 1994 that number was only 6,587,885. This indicates a dramatic increase in the number of heavy vehicles. In 2002, 434,000 large trucks were involved in traffic accidents. Of those accidents 4542 involved fatalities [1]. Given the dramatic increase in heavy truck use as well as the large number of accidents and fatalities every year involving heavy trucks, increasing attention is being given to the study of heavy truck crashworthiness and safety.

Heavy trucks can also be involved in rollover accidents. This type of accident, as is the case with passenger vehicles, is not as likely as other types of accidents, but can result in significantly more damage to the vehicle and injuries to the occupants of the heavy truck.

This paper describes a study of the heavy truck accidents that occurred in the time period from 1994-2002. The data was collected from the FARS database, which is controlled by NHTSA [2]. The specific interest was to evaluate significant structural damage to the truck, and injuries that occurred to the restrained occupants of the large trucks during rollover accidents. The crashworthiness of large trucks is briefly examined. A case study of a heavy truck rollover is also presented.

DATA SELECTION

Several databases exist that can be queried for specific accident data. The University of Michigan Transportation Research Institute compiles statistical data for heavy trucks; however, they do not provide the specific data that was of interest in this study. The FARS database was chosen because of the high specificity that can be used in developing a query. The data of greatest interest was that which could be used to determine the injuries of large truck occupants during a rollover accident. The specific data of interest is described in the abstract of this paper. The chosen delimiters could be selected to create a query for the FARS database.

DATA ANALYSIS

All heavy truck accidents were first evaluated and then the previously stated rollover query was used. From a comparison of these two queries, the percentage of fatal and incapacitating accidents that correspond to the specific rollover accident in question could be determined.

Figure 1 shows the results of all accidents from 1994-2002. The number of fatal accidents per year for heavy trucks peaked in 1999 at 659. The lowest number of fatal accidents for this time period was 523, which occurred in 1996. A downward trend is apparent from 1999-2002, with only 537 fatal crashes occurring in 2002. Since this data looks at all fatal heavy truck accidents, the number of vehicles and persons involved are somewhat higher every year than the number of fatal accidents.

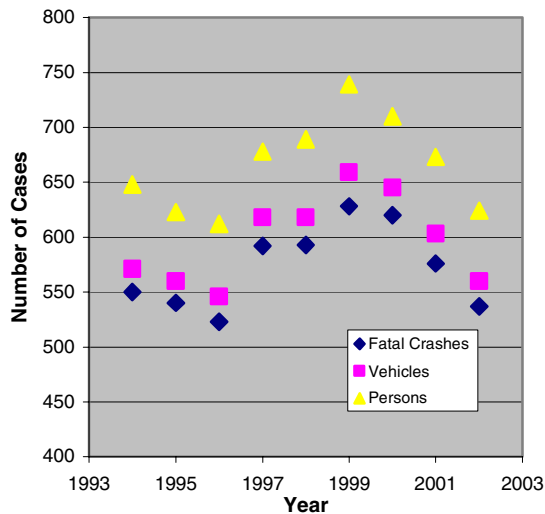


Figure 1. FARS data for all fatal and incapacitating heavy truck crashes from 1994-2002.

The rollover query was then submitted to the FARS database and the number of accidents that met the requirements of this query is shown in Figure 2. The average percent of fatalities and incapacitating injuries, which matched the rollover query, was 18%, with a high in 2002 of 21% and a low of 17% occurring in 1994, 1995, and 1997. Therefore, on average, 18% of all heavy truck incapacitating and fatal injuries were a result of a single vehicle rollover accident where the rollover was the most harmful event, either the first or subsequent event with contained occupants receiving fatal or incapacitating

injuries and the truck receiving severe and disabling damage. This is a very high percentage given such a specific type of accident.

The rollover data shown in Figure 2 shows some similar trends as the data for all heavy truck accidents shown in Figure 1. The highest number of fatal and incapacitating crashes, 126, occurred in 1998, with the lowest number of crashes, 93, being reported in 1993. A downward trend from 1998 to 2001 is seen, but in 2002 the number of crashes rose slightly from 107 in 2001 to 115 in 2002.

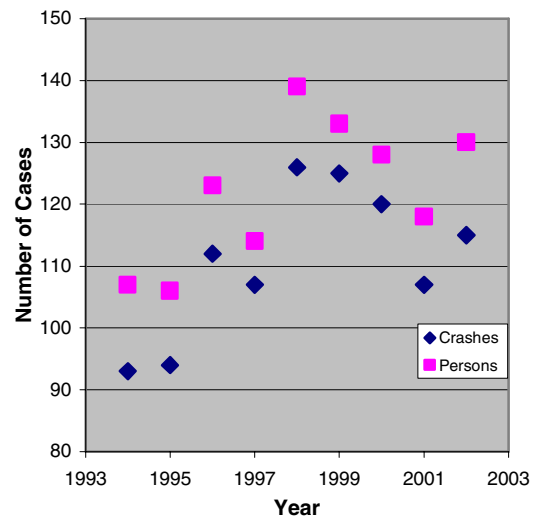


Figure 2. FARS data for heavy truck rollover accidents from 1994-2002 that meet the described query.

The results from the rollover query were further analyzed to determine the restraint use for these accidents. Table 1 shows the findings of this analysis. The average known restraint use during the 1994-2002 time period was almost 35% per year. The conclusion can be made from this data analysis that, on average, over 6% per year of all heavy truck fatalities and incapacitating injuries were restrained occupants in rollover accidents per the previously mentioned query.

Table 1.
Total fatalities and incapacitating injuries and percentage restrained in rollover accidents

Year	Total Incapacitated and Fatally Injured	Total Restrained Fatalities and Incapacitating Injuries	Percentage Restrained
1994	107	31	29.0
1995	106	35	33.0
1996	123	41	33.3
1997	114	44	38.6
1998	139	37	26.6
1999	133	48	36.1
2000	128	50	39.1
2001	118	44	37.3
2002	128	48	37.5

The overall conclusion from this data is that over 6% of the heavy truck incapacitating injuries and fatalities occur as a result of restrained occupants being killed or incapacitated from the severe or disabling deformation that occurs to the truck during a rollover accident.

ROLLOVER CRASHWORTHINESS

In 1991, UMTRI researchers Campbell and Sullivan reported at the 35th Stapp Car Crash Conference that about 60% of all heavy truck driver fatalities are associated with rollover accidents. They concluded from studying National Transportation Safety Board crash reports that, “Existing cab structures above the plane of the dash are not sufficient to withstand the forces produced during rollover” [3].

Several studies have been conducted to evaluate the crashworthiness of heavy trucks. Clarke and Leasure state that improving cab design to provide occupant survival space in a crash could enhance truck occupant protection [4]. In another crashworthiness study, Ranney concluded that heavy truck rollovers were the most frequent cause of truck occupant fatality and that the most frequent damage location in fatal rollovers was the top of the truck [5]. In 1978 Grattan and Hobbs of the United Kingdom conducted a study on injuries received by heavy truck occupants, from which they made the conclusion that making the cab more resistant to the crushing of its occupants could add to the protection offered by the seat belt [6].

Numerous other studies not mentioned have evaluated the injuries received during various types of heavy truck accidents. One conclusion can be drawn: insufficient survival space during rollover

accidents is a primary cause of death for the drivers of large trucks; therefore, structural integrity of the cab of the heavy truck is critical to occupant safety.

CASE STUDY

A seat-belted driver of a heavy truck was killed as a result of the structural collapse of his 1999 Freightliner FLD tractor cab during a 180° rollover accident. His truck was pulling a trailer carrying a full load of cylindrical hydrogen tanks. The rollover was precipitated by the impact of a full-size pick-up which swerved to the left, and struck the Freightliner truck, disabling the right steering mechanism. The Freightliner veered to the left and back to the right, eventually overturning and landing on the vehicle’s left side. The tractor and trailer slid down the roadway and started to slide onto the grassy shoulder to the right of the road. The tractor rolled onto its roof in the grass causing complete collapse of the cab. A photo of the accident vehicle is shown in Figure 3. The truck and trailer left the road and came to rest mostly parallel to the direction of traffic, with the trailer having crossed a driveway, and the cab resting on the driveway. According to the accident reconstruction, the speed of the tractor and trailer at the point of roll initiation was calculated to be in a range from 57 to 70 mph. The speed as the trailer exited the roadway was calculated to be approximately 35 mph.



Figure 3. Photograph of the accident vehicle – driver’s side.

The heavy truck suffered significant structural collapse during this rollover accident. The authors conducted an inspection of an exemplar vehicle and concluded that the all aluminum cab structure would not be sufficient for occupant protection in rollover accidents.

CONCLUSIONS

The FARS database was queried and data gathered for large truck rollover accidents. A specific query was designed to include rollover accidents of heavy trucks where the rollover was the most harmful event; the rollover was either the first or subsequent event; the truck received severe and disabling deformation; the occupants were not ejected; and the injuries sustained were either incapacitating or fatal. This rollover accident data was also compared with the total number of heavy truck accidents where incapacitating or fatal injuries occurred as reported by FARS for the 1994-2002 time period. This data was also then analyzed for restraint use. The following conclusions were made from this data analysis and review of a case study:

1. The average percent of persons involved in accidents, which matched the rollover query, was 18%, with a high in 2002 of 21% and a low of 17% occurring in 1994, 1995, and 1997.
2. The average yearly percentage of incapacitating and fatal injuries for restrained occupants was determined by analyzing the rollover data obtained from the FARS query and was found to be 35%.
3. The overall conclusion from this data is that over 6% of the heavy truck fatalities and incapacitating injuries occur as a result of restrained occupants being killed or incapacitated from the severe or disabling deformation that occurs to the truck during rollover accidents.
4. As stated by Campbell and Sullivan [3] and as was seen from the case study, "Existing cab structures above the plane of the dash are not sufficient to withstand the forces produced during rollover."

REFERENCES

[1] National Highway Traffic Safety Administration. 2002. "Traffic Safety Facts 2002: Large Trucks." DOT HS 809 608, National Center of Statistics and Analysis.

[2] National Highway Traffic Safety Administration, Fatality Analysis Reporting System (FARS) Web-Based Encyclopedia, <http://www-fars.nhtsa.dot.gov/>

[3] Campbell, K.L. and K.P. Sullivan. 1991. "Heavy Truck Cab Safety Study." Proceedings of the 35th Stapp Car Crash Conference. SAE Technical Paper 912903, 199-225.

[4] Clarke, R.M. and W.A. Leasure Jr. 1985. "Vehicle Factors in Accidents Involving Medium and Heavy Trucks." SAE Technical Paper 876086. 642-655.

[5] Ranney, T.A. 1982. "Injury Causation and Heavy Truck Occupant Crash Protection." 26th Annual Proceedings, American Association for Automotive Medicine, October 4-6. Ottawa, Ontario, Canada, 149-165.

[6] Grattan, E. and J.A. Hobbs. 1978. "Injuries to Occupants of Heavy Goods Vehicles." The Laboratory Report 854, Transport and Road Research Laboratory, Department of Transport, Crowthorne, Berkshire, United Kingdom.

DYNAMIC ROOF CRUSH INTRUSION IN INVERTED DROP TESTING

Stephen A. Batzer, Ph.D., P.E.

Renfroe Engineering, Inc.

United States of America

Robert M. Hooker

Eliseco Systems

United States of America

Paper Number 05-0146

ABSTRACT

Inverted drop testing of vehicles is a destructive determination of roof strength used by industry, government organizations and independent engineers to determine vehicle safety with respect to rollover collision. In this paper, the results of numerous inverted drop tests are summarized and analyzed, giving both the amount of permanent and temporary roof crush that occurs during impact. Only unmodified production vehicles with sound roofs were tested. The amount of dynamic roof crush varied from a low of 0 to a maximum of 7.0 cm, the relationship between elastic and plastic roof crush was not found to be statistically significant, and prediction intervals for A and B-pillar crush were developed.

INTRODUCTION

Many engineers believe that strong roofs provide significant protection to occupants during rollover collisions. As of this writing, the American National Highway Traffic Safety Administration (NHTSA) has opened docket #5572 regarding review of the technical methodology for certifying the roof strength of passenger vehicles. In this docket can be found arguments in support of, and counter-arguments dismissive of, the assertion that stronger roofs (beyond a certain minimal point) are safer roofs. This paper addresses the lack of solid data regarding impact-generated dynamic intrusion into the occupant space.

There is currently a lack of information regarding the dynamic intrusion of the roof structure into the occupant capsule as a result of rollover. This information has not been tabulated as a result of Family of Motor Vehicle Safety Standards (FMVSS) 216 tests, and cannot be reliably measured from actual rollover collisions. In some cases, evidence of dynamic intrusion is present due to witness marks on

headrests and other components during rollovers, but the actual intrusion distance still must be estimated rather than measured.

STATIC ROOF CRUSH TESTING

Roof strength is regulated in the United States by the FMVSS 216 standard, *Roof Crush Resistance – Passenger Cars*, and was adopted on September 1, 1973. General Motors developed the procedure at their research laboratories. One reason that it was adopted was for its repeatability, a desirable attribute for expensive, time-consuming tests.

The pre-amble of the FMVSS-216 standard states, “The purpose of this amendment...is to add a new Motor Vehicle Safety Standard...that sets minimum strength requirements for a passenger car roof to reduce the likelihood of roof collapse in a rollover accident” (emphasis added). As was alluded to in the introduction, there is significant, ongoing controversy regarding roof crush as it relates to occupant injury. Certainly, if roof crush is an issue in occupant safety, it is immaterial as to whether or not the intrusion that may or may not have injured the occupant was temporary or permanent.

DYNAMIC ROOF CRUSH TESTING

The quasi-static roof crush test mandated by the FMVSS 216 subjects the vehicle to a maximum force significantly less severe than would be applied to the vehicle during a multiple rollover. The Society of Automotive Engineers (SAE) recommended practice J996, *Inverted Drop Test*, is also a test of rollover crashworthiness, and was developed by SAE in the late 1960s. Since it is a more severe test, numerous engineers prefer it to the quasi-static FMVSS 216 test.

The SAE J996 test was designed, "...to obtain as closely as possible deformation of a vehicle roof or roll bar structure which occurs in a vehicle rollover." In this test, the subject vehicle is inverted, given a roll angle, pitch angle, and drop height that are representative of the assumed loading at rollover. The angles present ensure that the majority of potential energy is transferred directly to the A-pillar structure. This standard does not specify any crush measurement methodology, permanent or dynamic.

DEVICE DESIGN AND TEST PROCEDURE

A reusable telescoping rod assembly was designed and constructed to document dynamic crush. The two rods are made of cold-rolled 4130 steel, approximately 56 cm in length, with a 2 cm nominal inner diameter of the thin-wall hollow (female) upper rod, and a 2 cm nominal exterior diameter of the solid (male) lower rod. The rods are not spring loaded, but free to move axially in extension and compression. The rod ends are capped with machined gimbals that fit into bases to allow rapid re-orientation of the rod ends during testing thus preventing binding. The orientation of the rod assembly inside of the vehicle is such that it is perpendicular to the test pad as the vehicle is inverted and ready to be dropped. The driver's seat is removed or modified as necessary to accommodate rod mounting. The top base is riveted into place at the root of the pillar / roof rail interface, and the bottom base is welded to the floor or seat structure.

Once the device is in place, its installed length is measured, and a rubber o-ring is positioned at the exterior mating rim of the female rod. As the rod compresses during impact, the o-ring is displaced by the female rod. As the roof rebounds, the o-ring remains in place. By measuring the distance between the o-ring and the female rod, the amount of dynamic roof crush is determined. In some configurations of this dynamic roof crush measurement device, an ink marker is affixed to the female rod and the tip bears against the male rod in order to provide further visual documentation of relative rod travel. These two measurements were always found to be in agreement. Thus, this simple device documents both permanent (plastic) and dynamic (elastic) deformation of the roof. The rod is examined for free travel before and after testing to ensure no binding has occurred.

RESULTS AND STATISTICAL ANALYSIS

A compilation of the drop testing results is given in Table 1, given in Appendix I. Measurements were made to the nearest sixteenth of an inch, but have been given in SI units to the nearest millimeter. The amount of plastic intrusion for the A pillar varied from a low of 8.3 cm to a high of 42.5 cm, while the elastic varied from 0 - 6.4 cm. The amount of plastic intrusion for the B pillar varied from a low of 3.2 cm to a high of 40.6 cm, while the elastic varied from 1.3 - 7.0 cm. The average dynamic roof crush for both pillars was found to be approximately 4.4 cm.

Figure 1 shows the plastic roof crush plotted against the drop height for both the A and B pillars. As can be seen, the amount of plastic roof crush is not strongly correlated with drop height. These figures show the effect of differing roof strengths across different vehicle designs.

Figure 2 shows two graphs of elastic versus plastic roof crush for both the A and B-pillars. Importantly, there is no apparent trend linking the two different crush types. If least-squares regression lines were added to the plots, they each would show only a very modest positive slope. Calculations reveal that the confidence intervals on these two slope magnitudes includes zero, meaning that there is no statistically significant relationship between the two types of crush.

Figure 3 shows that A & B pillar plastic crush are strongly correlated. As expected, as the A pillar plastic crush increases, the B pillar residual crush also increases. The A-pillar plastic crush was always measured to be greater than that of the B-pillar plastic crush, although sometimes the two values differ only slightly. The average difference between the measurement sites was found to be 5.0 cm. The regression of the B pillar crush on to A-pillar crush is:

$$\hat{B} = 1.13A - 3.06 \quad (1)$$

where \hat{B} is the predicted residual B-Pillar crush, and A is the measured A-pillar plastic crush. The regression yields an $R^2 = 0.958$. This equation shows that there is an approximate 3 cm crush threshold for the A pillar to induce crush at the B pillar.

As was shown in Fig. 2, the elastic and plastic crush intrusions are not strongly correlated. It is, however, worthwhile to construct a prediction interval for the amount of elastic intrusion that is independent of the

plastic crush. That is, *if another drop test were performed for a randomly selected FMVSS-216 compliant vehicle, what interval of elastic intrusion values would bracket the next measured value with a 90% success rate?* Thus, if it is sensible to model crush measurements from the population of FMVSS-216 compliant vehicles as normally distributed, one may use the sample means and sample standard deviations from Table 1 to state such intervals predicting next measured values. Figure 4 shows Q-Q plots for the A and B pillar dynamic crush measurements. The data appears sufficiently “well behaved” to use a standard prediction limit interval analysis. A 90% prediction interval on the elastic intrusion is made as follows [Vardeman and Jobe, 2001]:

$$\bar{x} \pm t_{v, 1-\frac{\alpha}{2}} s \sqrt{1 + \frac{1}{n}} \quad (2)$$

where $v = n-1$, $n =$ sample size, and $\alpha = 0.90$. This yields two prediction intervals for the dynamic A-Pillar (3) and dynamic B-Pillar intrusion crush:

$$0 \text{ cm} < A_{0.90} < 8.4 \text{ cm} \quad (3)$$

$$1.3 \text{ cm} < B_{0.90} < 8.1 \text{ cm} \quad (4)$$

The A-pillar dynamic intrusion is of greater consequence, as the front seats are more likely to be occupied, and the plastic intrusion of the A-pillar is usually greater than that of the B-pillar in rollover collisions. The FMVSS-216 requires that the vehicle does not exceed 12.7 cm plastic intrusion during quasi-static testing. An 8.4 cm dynamic intrusion into the occupant survival space is a significant fraction of this allowable plastic deformation level.

CONCLUSIONS

During rollover collisions, energy is dissipated at a relatively low rate, making these events much less severe from the point of view of the vehicle than are other types of collision such as frontal impact. Franchini [1969] discussed the “crash survival space” which needs to be maintained for occupant survival. The volume of interior space enveloping the occupant represents the survival space, and takes into account the size, posture and position of the occupant. It is of principal importance in designing a vehicle for crashworthiness. An analysis of the testing presented in this paper sheds new insight into the integrity of the occupant survival space during

rollover collisions. It has been shown for the sample set presented that the measured crush at the A pillar exceed that at the B pillar, that the dynamic crush averaged approximately 4.4 cm, and that the amount of plastic and elastic crush are not strongly enough correlated for the relationship to be statistically significant for our sample size. Further, a 90% prediction interval for the elastic intrusion of FMVSS-216 compliant vehicles encompasses 0 – 8.4 cm at the A-pillar, and 0 – 8.1 cm at the B-pillar.

ACKNOWLEDGEMENTS

The authors express their sincere gratitude to Dr. Stephen B. Vardeman of the Iowa State University for his work in reviewing the statistical analysis presented in this manuscript.

REFERENCES

- [1] Federal Motor Vehicle Safety Standards; Roof Crush Resistance, Federal Register, Vol. 66, No. 204, pp. 53376-53385.
- [2] Franchini, E., “Crash Survival Space is needed in Vehicle Passenger Compartments,” SAE 690005.
- [3] Grymes, Christie L., and Collier Shannon Scott, “Product Demonstrations,” Doc. 567140, Ver. 1, 6/4/01.
- [4] SAE J996, “Inverted Vehicle Drop Test Procedure,” August, 1967.
- [5] Vardeman, S. B., and J. M. Jobe, “Basic Engineering Data and Analysis, Duxbury – Thomson Learning, 2001.

CONTACT INFORMATION

Dr. Steve Batzer is the senior forensic engineer of *Renfroe Engineering, Inc.* He can be reached at Renfroe Engineering, Inc., 13045 W. Hwy 62, Farmington, P.O. Box 610, AR, 72730, telephone 479-846-8000; fax 479-846-8002; email batzer@renfroe.com.

Mr. Robert Hooker is the founder and president of *Eliseco Systems*, a Michigan-based automotive testing facility. He can be reached at Eliseco Systems, 2046 School Road, Weidman, MI, 48893; telephone 989-644-8999; fax 989-6444-8990.

APPENDIX I – DATA

TABLE I: Plastic and dynamic roof crush measurements.

Make	Model	Year	Roll (°)	Pitch (°)	Drop Height (cm)	Plastic Crush (cm)	Dynamic Crush (cm)	Total Crush (cm)	Location
Ford	Aerostar	1993	25	5	30.5	19.7	5.1	24.8	A Pillar
Ford	Aerostar	1993	25	5	30.5	11.7	5.1	16.8	B Pillar
Ford	Bronco II	1984	25	5	30.5	32.4	6.4	38.7	A Pillar
Ford	Bronco II	1984	25	5	30.5	27.5	5.4	32.9	B Pillar
Ford	F-150	1986	25	5	30.5	42.5	6.0	48.6	A Pillar
Ford	F-150	1986	25	5	30.5	40.6	6.4	47.0	B Pillar
Honda	Accord	1988	25	5	45.7	21.3	4.4	25.7	A Pillar
Honda	Accord	1988	25	5	45.7	10.8	4.1	14.9	B Pillar
Hyundai	Excel	1991	25	5	30.5	21.9	4.8	26.7	A Pillar
Hyundai	Excel	1991	25	5	30.5	17.8	5.1	22.9	B Pillar
Isuzu	Rodeo	1994	25	5	30.5	12.4	1.7	14.1	A Pillar
Isuzu	Rodeo	1994	25	5	30.5	8.9	5.4	14.3	B Pillar
Nissan	Pickup	1985	25	5	30.5	34.6	0.0	34.6	A Pillar
Nissan	Pickup	1985	25	5	30.5	34.5	2.5	37.0	B Pillar
Plymouth	Laser	1992	25	5	30.5	10.2	6.4	16.5	A Pillar
Plymouth	Laser	1992	25	5	30.5	3.2	7.0	10.2	B Pillar
Pontiac	Fiero	1986	25	5	45.7	8.3	3.2	11.4	A Pillar
Pontiac	Fiero	1986	25	5	45.7	3.8	3.2	7.0	B Pillar
Subaru	Loyale	1993	25	5	30.5	17.8	1.3	19.1	A Pillar
Subaru	Loyale	1993	25	5	30.5	11.4	1.3	12.7	B Pillar
Suzuki	Samurai	1988	45	0	91.4	22.9	6.4	29.2	A Pillar
Suzuki	Samurai	1988	45	0	91.4	19.1	6.7	25.7	B Pillar
					\bar{X}	22.2	4.1	26.3	A Pillar
					s	10.2	2.2	10.4	
					\bar{X}	17.2	4.7	21.2	B Pillar
					s	11.7	1.7	11.8	

APPENDIX II – Statistical Analysis Graphs

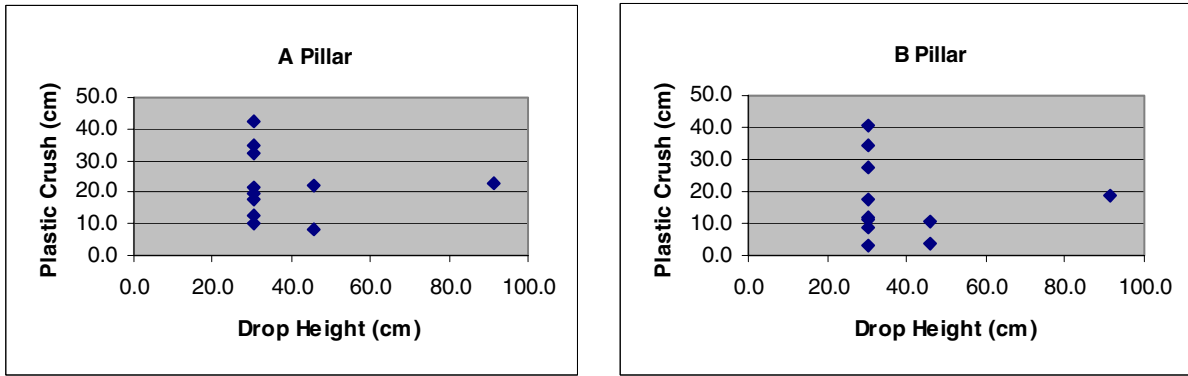


Figure 1. Plastic crush versus drop height for the A-Pillar.

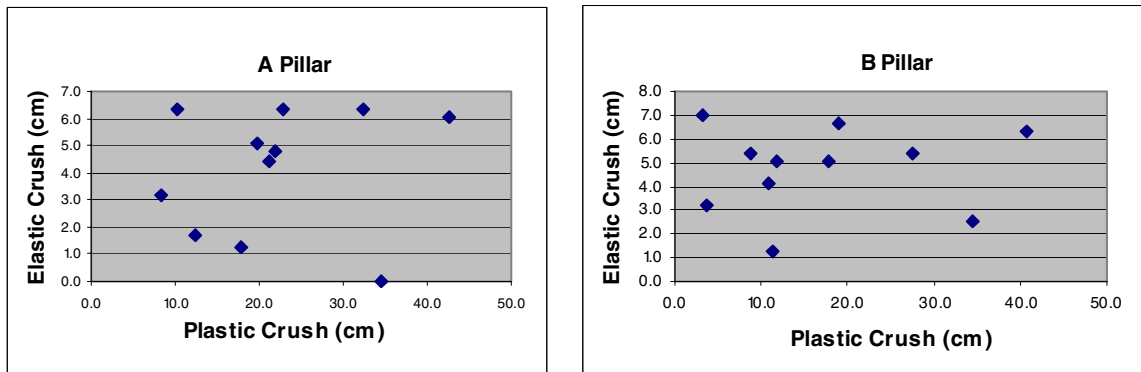


Figure 2. Elastic vs. plastic crush measurements.

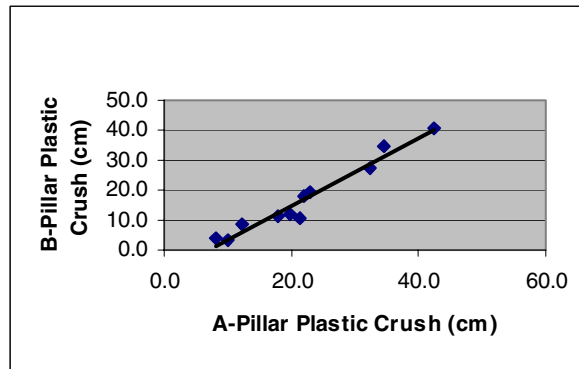


Figure 3. B vs. A pillar plastic crush.

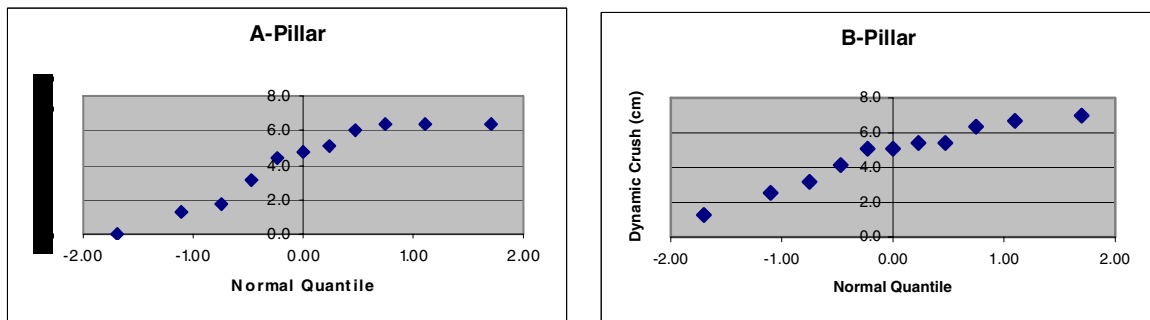


Figure 4. Q-Q Plots – A & B pillars.

A METHOD TO EVALUATE DYNAMIC vs. RESIDUAL ROOF RAIL DEFORMATION IN DOLLY ROLLOVER TESTS

John E. Cochran, Jr.

Auburn University
United States

Martha W. Bidez

University of Alabama at Birmingham
United States

Dottie King

Three Sigma, Inc.
United States

Paper Number 05-0378

ABSTRACT

The purpose of this study was to develop the analytical methodology to evaluate the dynamic versus residual roof deformation characteristics of a compact SUV subjected to SAE J2114 dolly rollover tests. Two FMVSS 208 dolly rollover tests with instrumented, restrained driver side Hybrid III dummies were evaluated during the first driver's side roof rail ground strike. Kinematic targets were mounted on the driver dummy head and tracked via onboard cameras as a means of visual validation of roof rail deformation (assuming rail-to-dummy head contact). Test instrumentation included: accelerometers at the vehicle center of gravity (CG), roof rail, pillars and rocker panel, lap and shoulder belt load transducers, triaxial accelerometers at the center of gravity of the head, chest and pelvis of the dummies and six-axis force (and moment) transducers in the neck of the dummy. All data was recorded consistent with SAE J211-1 recommendations

Vehicle angular velocity and attitude were estimated using the data from multiple accelerometers, which correlated well with the test video. The accelerometer data indicate that the driver roof rail dynamic deformation was significantly greater than the residual deformation to which the roof rail rebounded following loss of ground contact. The dynamic deformation was of such magnitude that the rail intruded into the driver's occupant survival space. A spike in driver dummy head acceleration was observed immediately following the acceleration pulse that caused the rail intrusion. The presence of significant *dynamic* roof rail deformation is new and important quantitative information that should be added to the body of knowledge surrounding reconsideration of FMVSS 216 and catastrophic injury prevention in rollover crashes.

INTRODUCTION

Rollovers present a high degree of risk to occupants as evidenced by the fact that rollovers have a higher fatality rate than other kinds of crashes. Of the nearly 11 million passenger car, SUV, pickup and van crashes in 2002, only 3% involved a rollover. However, rollovers accounted for nearly 33 out of every 100 deaths from passenger vehicle crashes. This is an astonishingly high figure. In 2002 alone, more than 10,000 consumers died in rollover crashes. (NHTSA, 2003) An even higher number of consumers were critically injured in rollovers, which translates into hundreds of millions of dollars of unnecessary health care costs on society in general.

A debate between safety professionals and industry representatives over whether roof crush causes catastrophic injury or whether it is simply associated with the injury has been ongoing for almost two decades. Within the rollover environment, the dynamic motion of a vehicle's roof rail at first ground strike, prior to the effects of multiple ground strikes and cumulative structural damage, provides an opportunity to study its influence on dummy kinematics and injury measures.

During the nine month interval from December 9, 1998 to August 11, 1999, Ford Motor Company sponsored a number of J2114 dolly rollover tests of Explorer vehicles at Autoliv ASP (Auburn Hills, MI). The structures of the SUVs were instrumented with accelerometers at the vehicle's center of gravity and all pillars, roof rails and rocker panels. Two fully instrumented Hybrid III 50th percentile male dummies were three-point restrained in the driver and right front passenger seating positions. A total of 118-127 channels of data as well as external and internal video footage were collected for each test.

In 2003, the full raw data set was made available for our review and analysis in litigation involving

consumers injured in rollover crashes involving Ford SUVs. An overview of the data was presented to NHTSA by representatives of Ford on March 5, 2004, and publicly posted in the docket (NHTSA-1999-5572-61) on April 13, 2004. Ford's public presentation of the Autoliv data was, to the best of our knowledge, Ford's first public release of the test data, which fortunately allowed the scientific community public access to information that had previously been kept confidential.

The purpose of this study was to develop the analytical methodology to evaluate the dynamic versus residual roof deformation characteristics in the Autoliv SUV dolly rollover tests using accelerometers mounted at the vehicle center of gravity (CG), roof rail, pillars and rocker panel. Dynamic neck loads of a lap-shoulder restrained Hybrid III 50th percentile male driver dummy were compared to the driver rail acceleration profile during the first driver's side roof rail ground strike. Kinematic targets mounted on the driver dummy head and tracked via onboard cameras provided a means of visual validation of the mathematical estimations of rail displacement. All sensor data was recorded and filtered consistent with SAE J211-1 recommendations.

Constitutive equations were derived to properly process the accelerometer output data into acceptable forms for testing for both mathematical reliability and biomechanical engineering validity related to occupant protection in rollovers. The equations used in this study describe a deformable body that is undergoing general translational and rotation motion as well as deformation. Six degrees of freedom are required for general translation and rotation and typically utilize a large number of degrees of freedom are needed to model deformation. However, because we are concerned, at the present time, with processing data from accelerometers fixed to various points on the vehicle, we did not, for the purposes of this study, need to consider the number of degrees of freedom used to model the deformation. We only needed to model the part of the acceleration due to the deformation appropriately. Hence, we developed kinematic equations for the relative motion of each sensor with respect to a common point for which we know the acceleration. Since these equations contain angular velocity and angular acceleration of the vehicle, we considered the problem of determining its rotational motion from the available data.

Kinematics

In Figure 1, the $Ox_Ey_Ez_E$ system is an "Earth-fixed" coordinate system which is fixed in location and orientation. The vector \vec{R}_C from O to C, the original center of mass of the vehicle, and the vector \vec{r}_7 locates a sensor denoted as "7" in the earth-fixed coordinate system. In the rollover tests, sensor S7 is a two-axis accelerometer at the B-pillar on the driver's side. The acceleration measured by sensor S7 is equal to the acceleration of the center of mass, C, of the vehicle, plus the acceleration of S7 relative to C, i.e., the acceleration due to rotation of the vehicle about C and the acceleration due to localized rail/pillar deformation.

This may be expressed mathematically as

$$\vec{A}_{S7} = \vec{A}_C + \vec{A}_{S7/C} \quad (1)$$

where \vec{A}_{S7} , \vec{A}_C , and $\vec{A}_{S7/C}$ are the accelerations of S7, C, and S7 with respect to C, respectively. It follows from (1) that the acceleration of S7 with respect to C is

$$\vec{A}_{S7/C} = \vec{A}_{S7} - \vec{A}_C \quad (2)$$

Since part of the acceleration of the sensors with respect to the center of gravity is due to the rotation of the vehicle, the angular velocity and angular acceleration of the vehicle-fixed axes must be used. Two methods were utilized in this investigation to determine the angular velocity, both with and without the use of a rollover sensor. If very good estimates of the angular velocity can be obtained then the vehicle's attitude may be obtained by numerical integration. Also, the parts of the accelerations of the sensors with respect to the center of gravity that are due to the rotation of the vehicle may be removed from equations like Eq. (2) and the part of the acceleration due only to deformation integrated to get deformation rates and displacements. Because each sensor has its own coordinate system, if the deformations are extreme (e.g. significant roof crush into the occupant survival space), then some method must be devised to account for the rotation of individual sensors.

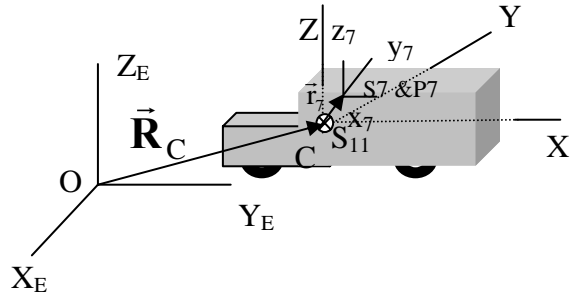


Figure 1. Earth-Fixed, Vehicle-Fixed, and Sensor Coordinate Systems.

If the components of $\bar{\mathbf{A}}_{S7/C}$ in the CXYZ system are used to calculate velocity and position, then the results should not contain the principal terms due to the translation of the center of mass of the vehicle. However, the rotation of the vehicle must still be properly included.

By definition, the acceleration $\bar{\mathbf{A}}_{S7/C}$ is the second time derivative of $\bar{\mathbf{r}}_7$. The latter may be written (See, for example, Meriam, 1971.) as

$$\bar{\mathbf{A}}_{S7/C} = \delta^2 \bar{\mathbf{r}}_7 / \delta t^2 + 2 \bar{\boldsymbol{\omega}} \times \delta \bar{\mathbf{r}}_7 / \delta t + \bar{\boldsymbol{\omega}} \times (\bar{\boldsymbol{\omega}} \times \bar{\mathbf{r}}_7) + \bar{\boldsymbol{\omega}} \times \bar{\mathbf{r}}_7 \quad (3)$$

where $\bar{\boldsymbol{\omega}}$ is the angular velocity of the CXYZ coordinate system and the derivative $\delta \bar{\mathbf{r}}_j / \delta t$ of a vector $\bar{\mathbf{r}}_j$ indicates the time derivative of that vector as seen in the rotating (vehicle-fixed) system CXYZ. The quantity $\delta^2 \bar{\mathbf{r}}_j / \delta t^2$ is the relative acceleration (acceleration as viewed by an occupant of the vehicle as he/she rotates with the vehicle-fixed CXYZ system) due to the deformation of the vehicle's structure at point P7 to which the sensor S7 is attached. Now, $\bar{\mathbf{r}}_7$ may be written as

$$\bar{\mathbf{r}}_7 = \bar{\mathbf{r}}_{70} + \delta \bar{\mathbf{r}}_7 \quad (4)$$

where $\bar{\mathbf{r}}_{70} = X_{70} \hat{\mathbf{I}} + Y_{70} \hat{\mathbf{J}} + Z_{70} \hat{\mathbf{K}}$ is the position vector of point P7 on the driver's roof rail/B-pillar in the vehicle-fixed CXYZ system when there is no deformation of the roof rail and $\delta \bar{\mathbf{r}}_7 = \delta X_7 \hat{\mathbf{I}} + \delta Y_7 \hat{\mathbf{J}} + \delta Z_7 \hat{\mathbf{K}}$ is the displacement of P7 due to local deformation ("crush") of the roof rail/B-pillar.

In most structures, under elastic deformation conditions, the displacements δX_7 , δY_7 , and

δZ_7 are related by the fundamental mode shapes of the structure. In the present case of a compact SUV, the deformation is a combination of elastic and plastic, dynamic and residual deformation types. An approach in which the displacements δX_7 , δY_7 , and δZ_7 are first considered to be independent and then the rotation of the sensor is estimated on the basis of the translation of the sensor appears to be reasonable.

Thus, assuming that there is little rotation of the vehicle's structure at P7 due to deformation, we may write

$$\delta^2 \bar{\mathbf{r}}_7 / \delta t^2 = \delta \ddot{X}_7 \hat{\mathbf{I}} + \delta \ddot{Y}_7 \hat{\mathbf{J}} + \delta \ddot{Z}_7 \hat{\mathbf{K}} \quad (5)$$

If the angular velocity $\bar{\boldsymbol{\omega}}$ and, hence, the angular acceleration $\dot{\bar{\boldsymbol{\omega}}}$, as functions of time are available from an angular velocity transducer and, if S7 and S11 are triaxial accelerometers, then estimates of δX_7 , δY_7 , and δZ_7 may be obtained from

$$\delta^2 \bar{\mathbf{r}}_7 / \delta t^2 = -2 \bar{\boldsymbol{\omega}} \times \delta \bar{\mathbf{r}}_7 / \delta t - \bar{\boldsymbol{\omega}} \times (\bar{\boldsymbol{\omega}} \times \bar{\mathbf{r}}_7) - \dot{\bar{\boldsymbol{\omega}}} \times \bar{\mathbf{r}}_7 + \bar{\mathbf{A}}_{S7/C} \quad (6)$$

Or, in matrix form for sensor S_j,

$$\ddot{\mathbf{r}}_j = -2 \tilde{\boldsymbol{\omega}} \dot{\mathbf{r}}_j - \tilde{\boldsymbol{\omega}} \tilde{\boldsymbol{\omega}} \mathbf{r}_j + \tilde{\mathbf{r}}_j \dot{\boldsymbol{\omega}} + \mathbf{A}_{Sj} - \mathbf{A}_C \quad (7)$$

where

$$\mathbf{r}_j = \begin{bmatrix} X_{j0} + \delta X_j \\ Y_{j0} + \delta Y_j \\ Z_{j0} + \delta Z_j \end{bmatrix}, \quad \boldsymbol{\omega} = \begin{bmatrix} \omega_x \\ \omega_y \\ \omega_z \end{bmatrix},$$

$$\tilde{\boldsymbol{\omega}} = \begin{bmatrix} 0 & -\omega_z & \omega_y \\ \omega_z & 0 & -\omega_x \\ -\omega_y & \omega_x & 0 \end{bmatrix}$$

and

$$\tilde{\mathbf{r}}_j = \begin{bmatrix} 0 & -(Z_{j0} + \delta Z_j) & (Y_{j0} + \delta Y_j) \\ (Z_{j0} + \delta Z_j) & 0 & -(X_{j0} + \delta X_j) \\ -(Y_{j0} + \delta Y_j) & (X_{j0} + \delta X_j) & 0 \end{bmatrix}$$

In Eq. (7), \mathbf{A}_C contains the components of the acceleration of the center of mass measured in the CXYZ system, while \mathbf{A}_{S_j} contains the components of the acceleration of sensor S_j measured in the $S_jx_jy_jz_j$ system. If there is relative rotation of these coordinate systems, then we must, of course, consider that if it is necessary.

Rotational Motion and Center of Gravity Position

Rotational Motion Obtained from Accelerometer Data

The data taken during Autoliv's Test B190042 include three-dimensional acceleration data from an accelerometer at the Visteon Fleet Roll Sensor, Autoliv Reference No. S1 [Ref. 1, page 18]. This additional data provides the relative acceleration of a third point in the vehicle that can be used to estimate the angular velocity and attitude of the vehicle. In the "vehicle-fixed" coordinate system, the sensor locations are identified by the respective position vectors of S1 (Visteon Fleet Roll Sensor, C.G.), S4 (Driver Rocker Panel Accelerometer at the B-pillar, DRPBP), and S9 (Passenger Rocker Panel Accelerometer at the B-pillar, PRPBP), which are

$$\bar{\mathbf{R}}_1 = 1635.00 \hat{\mathbf{I}}_G - 59.90 \hat{\mathbf{J}}_G + 961.00 \hat{\mathbf{K}}_G \text{ mm} \quad (8a)$$

$$\bar{\mathbf{R}}_4 = 2802.90 \hat{\mathbf{I}}_G - 768.10 \hat{\mathbf{J}}_G + 762.30 \hat{\mathbf{K}}_G \text{ mm} \quad (8b)$$

$$\bar{\mathbf{R}}_9 = 2833.70 \hat{\mathbf{I}}_G - 716.40 \hat{\mathbf{J}}_G + 750.70 \hat{\mathbf{K}}_G \text{ mm} \quad (8c)$$

Similarly, the global position vector of the center of gravity is

$$\bar{\mathbf{R}}_{C.G.} = 2073.10 \hat{\mathbf{I}}_G - 24.50 \hat{\mathbf{J}}_G + 975.00 \hat{\mathbf{K}}_G \text{ mm} \quad (9)$$

These points are shown in Figure 2.

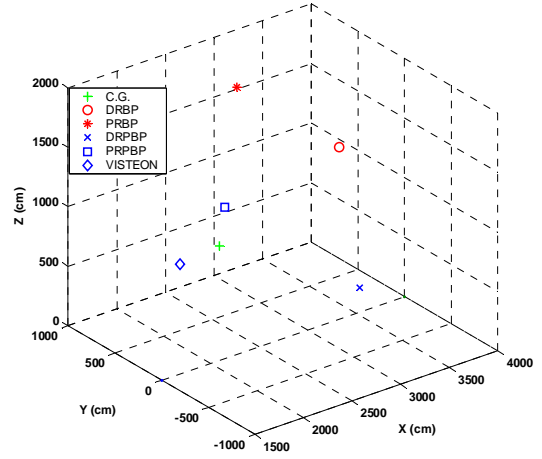


Figure 2. Six Sensor Locations for Autoliv Test B190042

The positions of the accelerometers with respect to the C.G. are

$$\bar{\mathbf{r}}_1 = -438.10 \hat{\mathbf{I}} - 35.40 \hat{\mathbf{J}} + 14.00 \hat{\mathbf{K}} \text{ mm} \quad (10a)$$

$$\bar{\mathbf{r}}_4 = 729.80 \hat{\mathbf{I}} - 743.60 \hat{\mathbf{J}} - 212.70 \hat{\mathbf{K}} \text{ mm} \quad (10b)$$

$$\bar{\mathbf{r}}_9 = 760.60 \hat{\mathbf{I}} + 740.90 \hat{\mathbf{J}} - 224.30 \hat{\mathbf{K}} \text{ mm} \quad (10c)$$

We can use the matrix form of the relative accelerations from the three accelerometers,

$$\ddot{\mathbf{r}}_j = -2\tilde{\omega} \dot{\mathbf{r}}_j - \tilde{\omega} \tilde{\omega} \mathbf{r}_j + \tilde{\mathbf{r}}_j \dot{\omega} + \mathbf{A}_{S_j} - \mathbf{A}_C, j=1, 4, 9 \quad (11)$$

and assume that the structural deformation is zero at each of the accelerometers to get

$$-\tilde{\mathbf{r}}_j \dot{\omega} = -\tilde{\omega} \tilde{\omega} \mathbf{r}_j + \mathbf{A}_{S_j/C}, j=1, 4, 9 \quad (12)$$

We have nine equations from which we can find $\dot{\omega}$, but because of the skew-symmetry of the $\tilde{\mathbf{r}}_j$, we have only six independent ones. Still these are more than we need to find, $\dot{\omega}$ so we use a weighted least squares approach. We pre-multiply the j th equation by $\tilde{\mathbf{r}}_j \mathbf{W}_j$, where \mathbf{W}_j is a constant, diagonal, 3×3 weighting matrix, and add the results to get

$$\mathbf{I} \dot{\omega} = -\tilde{\omega} \mathbf{I} \tilde{\omega} + \tilde{\mathbf{r}}_1 \mathbf{W}_1 \mathbf{A}_{S1/C} + \tilde{\mathbf{r}}_4 \mathbf{W}_4 \mathbf{A}_{S4/C} + \tilde{\mathbf{r}}_9 \mathbf{W}_9 \mathbf{A}_{S9/C} \quad (13)$$

In Eq. (13),

$$\mathbf{I} = -\tilde{\mathbf{r}}_1 \mathbf{W}_1 \tilde{\mathbf{r}}_1 - \tilde{\mathbf{r}}_4 \mathbf{W}_4 \tilde{\mathbf{r}}_4 - \tilde{\mathbf{r}}_9 \mathbf{W}_9 \tilde{\mathbf{r}}_9 \quad (14)$$

is analogous to the inertia matrix of a rigid body and the sensor terms are analogous to torques.

By using the weighting matrices

$$\mathbf{W}_1 = \begin{bmatrix} 1/2 & 0 & 0 \\ 0 & 1/2 & 0 \\ 0 & 0 & 1/2 \end{bmatrix} \quad (15a)$$

and

$$\mathbf{W}_4 = \mathbf{W}_9 = \begin{bmatrix} 1/2 & 0 & 0 \\ 0 & 1/2 & 0 \\ 0 & 0 & 1/2 \end{bmatrix} \quad (15b)$$

we obtained the time histories for the Test B190042 angular velocity components and Euler angles of the vehicle shown in Figures 3 and 4. The weights are somewhat arbitrary, but the sum should be 1. The Visteon accelerometer output was weighted more heavily than that of the other two sensors because such weighting gives better results for pitch and yaw.

Note that because the vehicle Z-axis is initially directed upward and the X-axis is rearward, a positive pitch angle puts the nose of the vehicle higher and a positive yaw angle means that the nose of the vehicle has rotated towards the left from the viewpoint of a driver. A positive roll angle is initially a rotation of the driver's side of the vehicle toward the ground.

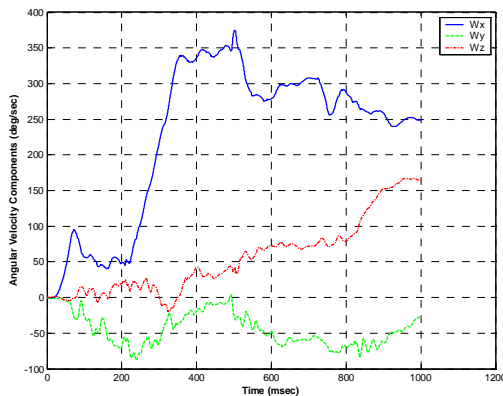


Figure 3. Estimated Angular Velocity Components – No Roll Rate Sensor Data (Autoliv Test B190042)

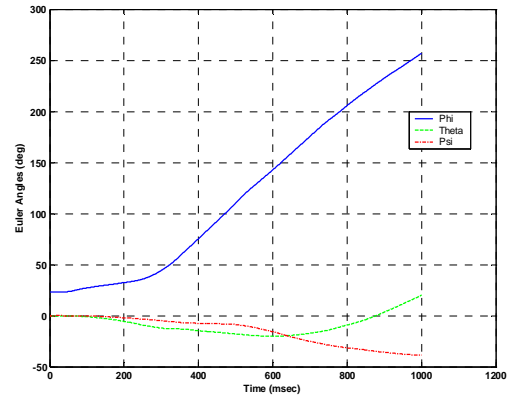


Figure 4. Estimated Euler Angles - No Roll Rate Sensor Data (Autoliv Test B190042)

Rotational Motion Obtained by Including the Systron Roll Rate Sensor Data

The data collected during Test B190042 included the output from the Systron Donner Roll Rate Sensor. Assuming that the “roll rate data” is actually the angular velocity about the X-axis of the vehicle, it may be used as the X-component of angular velocity in our estimate of angular velocity and the other two components may be obtained as indicated above. Figures 5 and 6 show the resulting time histories of the angular velocity components and the Euler angles. Note that the agreement between the time histories of the X-components of the angular velocity shown in Figure 3 and Figure 5 is very good except for the oscillatory content in ω_x in Figure 5. Because the rate data was used directly to obtain Figure 5, the ω_x time history shown there still has considerable oscillatory content. On the other hand, the ω_x plot in Figure 3, which was obtained by integrating the accelerometer outputs after they have been filtered (60 Hz), does not have the high frequency content.

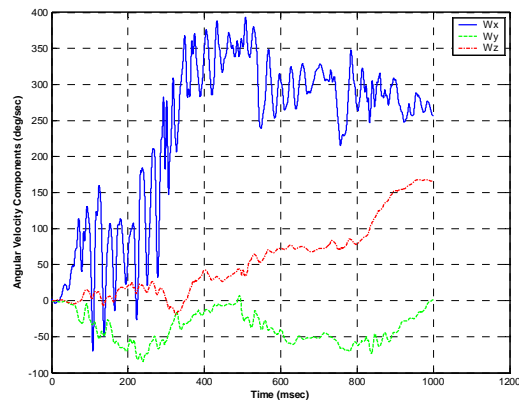


Figure 5. Angular Velocity Components Including Systron Roll Rate Sensor Data

The results for the Euler angles that were obtained using the four accelerometers (CG, DRPBP, PRPBP, and VISTEON) and the Systron Donner Roll Rate Sensor are presented in Figure 6. Note that the assumption was made that the Systron Donner sensor measures the angular velocity about the X-axis, not the time rate of change of the Euler angle ϕ (Phi).

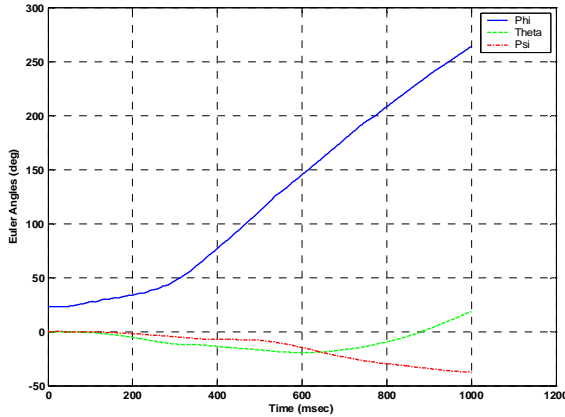


Figure 6. Estimated Euler Angles Including Systron Roll Rate Sensor Data.

Analysis of Data from B190043

Although it is SAE recommended procedure, it appears that in at least one Autoliv test (B190043) no angular velocity data was collected. Also, the accelerometer S7 provided only Y- and Z-accelerations in both Autoliv tests. The angular velocity, however, may be estimated in a test not providing angular velocity sensor data, by using the vehicle CG accelerometer (S11) and any two triaxial accelerometers that are positioned such that the three are not collinear (as described infra). Figure 7 presents such an estimate obtained using sensors S4 and S9. These two are not collinear with C. The estimates of angular velocity components are similar to those in the Controlled Rollover Impact System (CRIS) study. (Carter, 2002) However, shortly after 500 ms some large changes in acceleration occur and when used in the equation for B-pillar deformations, the values for angular velocity components seem to be too large. Fortunately, there is another way to estimate the dynamic crush using Eq. (7).

The terms due to angular velocity in Eq. (6) are fairly constant just before the acceleration in the B-pillar becomes very large. Thus, if the value of the right-hand side of Eq. (6) at time t_{start} before the large acceleration pulse is used as the part of $\delta^2 \vec{r}_7 / \delta t^2$

not due to the crushing, then the part of $\delta^2 \vec{r}_7 / \delta t^2$ due to deformation is

$$\delta^2 \vec{r}_7 / \delta t^2 \Big|_{\text{deformation}} \cong \bar{\mathbf{A}}_{S7}(t) - \bar{\mathbf{A}}_C(t) - [\bar{\mathbf{A}}_{S7}(t_{start}) - \bar{\mathbf{A}}_C(t_{start})] \quad (16)$$

Equation (16) may be integrated component by component if both sides are written in terms of unit vectors fixed in CXYZ. Figure 8 shows the results for the roof rail/B-pillar deflection/crush using this method. Thus, the direct integration of acceleration data provides meaningful results, if the data is chosen properly.

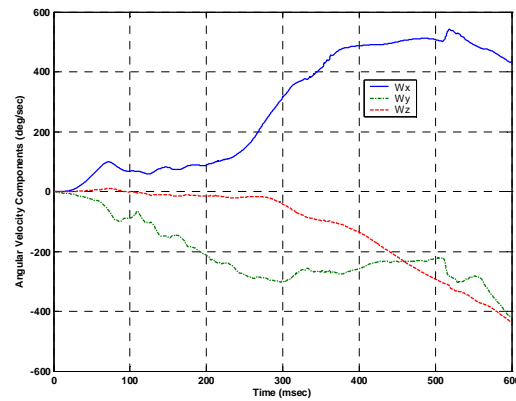


Figure 7. Angular Velocity Estimated from Accelerometer Data (Autoliv Test B190043)

The methodology described here can be used to obtain estimates of the dynamic motion when good estimates of the angular velocity of the vehicle are known from angular velocity transducers. Even without angular velocity data, dynamic crush can be estimated through judicious use of the accelerometer data by subtracting the more constant terms due to angular velocity. The estimates of 9 inches in Y-dynamic deformation and -3.5 inches in Z-dynamic deformation shown in Figure 8 are based on integrating the differential accelerations of the B-pillar over 200 ms. As shown in Figure 9, the integration of the differential accelerations starting at 500 ms actually produces a larger Y-dynamic deformation result of 10.5 inches and a slightly smaller magnitude negative Z-value of about -2 inches. These estimates compared well to the photogrammetric measurement of lateral roof deformation from the test video. Using the shorter period of time when the B-pillar was experiencing very high acceleration probably yields the better estimate. Since the Z-deformation is small, it

appears that the sensor rotated very little with respect to the vehicle-fixed coordinate system.

Of course, the data obtained in this manner provides a snapshot of the change in the deformation at a given time, and not the total crush time history. Since we are concerned with the relative motion of the parts of the vehicle, particularly with respect to restrained occupants, such results are very important.

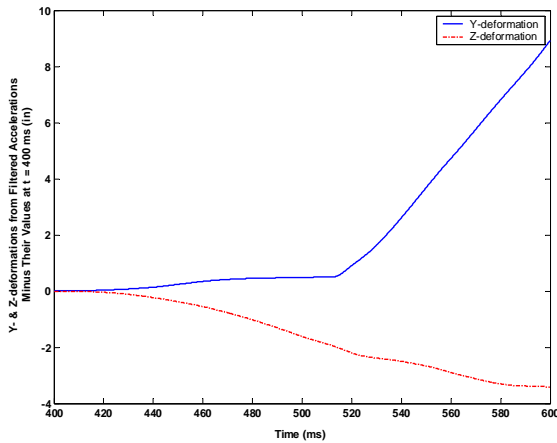


Figure 8. B-pillar Dynamic Deformations Integration Start at 400 ms. (Autoliv Test B190043)

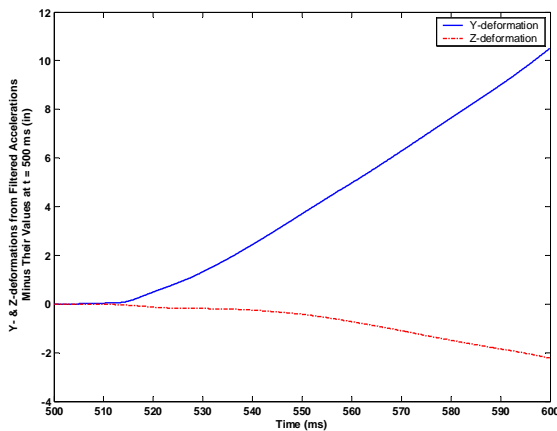


Figure 9. Y- and Z-deformations of the B-pillar Integration Start at 500 ms (Autoliv Test B190043)

CONCLUSIONS

A method has been developed for properly processing the SUV roof rail accelerometer output data into acceptable forms for testing for both mathematical reliability and biomechanical engineering validity related to occupant protection in

rollovers. The method has been implemented in the analysis of catastrophic injuries predicted by restrained driver and passenger dummies in FMVSS 208 dolly rollover tests (refer to the authors' submission to Docket No. NHTSA-1999-5572).

REFERENCES

Autoliv, ASP, "Final Report of SAE J2114 Rollover Crash Testing on Ford Explorer, Test Number B190043", Autoliv ASP Automotive Technical Center, 1320 Pacific Drive, Auburn Hills, MI 48326.

Brogan, W. L., Modern Control Theory, Quantum Publishers, Inc., New York, 1974, p. 92.

Carter, J. W., Habberstad, J. L., Croteau J., "A Comparison of the Controlled Rollover Impact System (CRIS) with the J2114 Rollover Dolly," SAE Paper No. 2002-01-0694, Reprinted From: Advances in Safety Test Methodology (SP-1664), SAE 2002 World Congress, Detroit, Michigan, March 4-7, 2002.

Fitz-Coy, N. G., and Cochran, J. E., Jr., Space Station/Shuttle Orbiter Dynamics During Docking, AAS 85-402, presented at the AAS/AIAA Astrodynamics Specialists Conference, Vail, Colorado, August 12-15, 1985.

Cochran, J. E., Jr., Cheng, Y-M, Bigelow, S., Sandidge, D., and Benner, J., "Multiple Body Missile Launcher Simulation," AIAA Paper 94-345, presented at the AIAA Atmospheric Flight Mechanics Conference, Scottsdale, AZ, August 1-3, 1994.

Henry, M. E., "Virtual Simulation of a Pickup Truck Rollover Test using the Nonlinear Finite Element Code PAM-CRASH," Pennsylvania State University, May 2003.

Mechanical Simulation Corporation, see www.carsim.com.

Meriam, J. L., Dynamics, Second Edition, John Wiley & Sons, Inc., New York, 1971, Chapter 2, Chapter 7.

NHTSA, <http://www.nhtsa.dot.gov/cars/problems/Rollover/characteristics/fatalities.htm>. November 24, 2003

REDUCING ROLLOVER OCCUPANT INJURIES: HOW AND HOW SOON

Donald Friedman and Carl E. Nash, Ph.D.

Center for Injury Research

United States

Paper No. 05-0417

ABSTRACT

Public release of previously confidential Malibu test data and film [1] provides the basis for this review. These are sixteen well-instrumented, definitive 32 mph dolly rollover tests of production Chevrolet Malibu sedans with unbelted Hybrid III dummies and eight with belted dummies (half of the cars in each group had roll cages to simulate strong roofs). This paper analyzes and reinterprets this material to resolve the principal motivating research question: does a strong roof reduce the potential for rollover head and neck injuries? Our findings are: (1) a rolling vehicle's center of gravity rises and falls only about 10 cm during a rollover so that its vertical velocity at roof impact is never more than 2.5 m/sec; (2) the six dummies showing the highest head and neck forces were all seated on the far side of Malibus without roll cages; (3) these high head and neck loads occurred after onset of roof intrusion from rapid roof collapse and buckling, not from occupant diving; (4) average roof impact neck forces measured by near side dummies and by far side dummies seated under roofs that did *not* contact the ground all averaged 3,300 to 3,600 N, and none was sufficient to cause serious injury; (5) the unrestrained Hybrid III dummy drop tests showed that neck loads of 7,000 N correspond to a 2.4 m/sec roof intrusion velocity while 3,500 N neck loads corresponds to a 1.1 m/sec intrusion velocity; (6) the windshields of the production vehicles broke early leaving weakened roof structures that deformed back and forth with subsequent roof impacts; and (7) the tempered side glazing of production Malibus broke far more frequently than in rollcaged vehicles facilitating partial or complete ejection. The Malibu tests provide considerable insight into the potential countermeasures that could reduce rollover injuries.

INTRODUCTION

In May 2004, General Motors finally released extensive data from the 1983-1990 Malibu tests [2,3] previously seen only in litigation. These data provide the most comprehensive information on rollover, dummy dynamics, and head and neck injury potential as a function of roof strength and occupant restraint available at this time. Because we question some aspects of the analyses conducted by the engineers

who conducted the tests, we have conducted a detailed re-analyses of the Malibu data.

Two SAE papers, referred to as Malibu I and II, reported on the two test series of dolly rollover tests of 1983 Chevrolet Malibu sedans. Malibu I was conducted in 1983 and reported in papers published in 1985. In these tests, two unbelted Hybrid III dummies were in the driver and right front passenger positions in the Malibu sedans. Four of these vehicles were production models, and four had strong roll cages installed in them that emulated a strong roof, substantially limiting roof crush. Malibu II was conducted in 1987 and reported in 1990. These tests were identical to the Malibu I tests except that they were conducted with lap and shoulder belted dummies where the belts had cinching latch plates.

These are the definitive tests for understanding the role of roof performance in occupant head and neck injury. These dolly rollover tests demonstrate that:

- The most severe neck injuries (i.e. the highest axial, shear, and moment neck loads) occurred to dummies seated on the far (initially trailing) side in roof impacts of production Malibus without roll cages. Taking other evidence of human neck tolerance, only these six exceeded a conservative axial neck load criterion (7,000 N): all were in Malibus with production roofs. These are shown in Figures 1 and 2 where the forces are converted to the head to roof contact velocity by photo-analysis to an accuracy of + or - 10%. The highest HIC, 2,820, occurred from a 20 mph buckling roof intrusion in Malibu I impact 1L3 in a production Malibu (a HIC above 1,000 is considered to be indicative of a high probability of serious head injury).
- The center of gravity of a rolling vehicle does not rise or fall more than a few inches during a rollover. Thus, the vertical velocity of the center of gravity of the vehicle at roof impact is low - virtually never more than 2.5 m/sec (5 mph). This is a survivable impact speed for a human head/neck, particularly if there is padding in the roof as is now required by FMVSS 201. The basis for this claim is the production and roll caged vehicle plots in Malibu I of the motion of the CG in the vertical, horizontal and rotational directions. We have previously shown that the vertical falling velocities of the sequence of near and far side roof

rollover impacts were similar and about 1 mph in production and about 3 mph in roll caged vehicles as shown in Figures 3 and 4 [4].

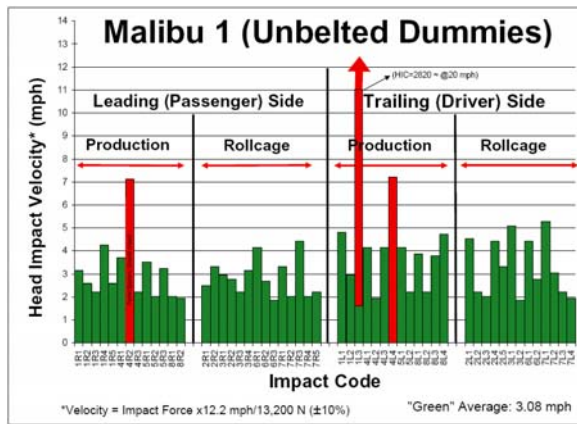


Figure 1. Malibu I neck compression velocities.

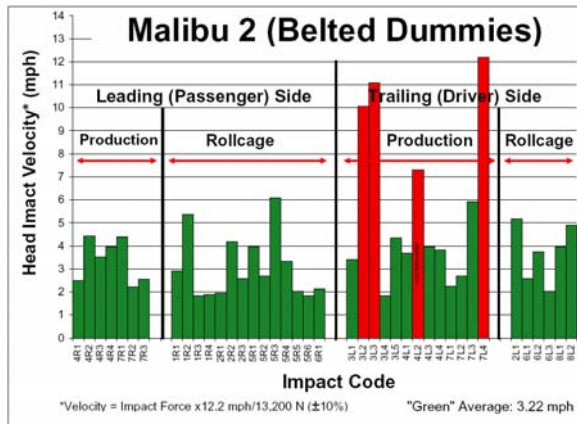


Figure 2. Malibu II neck compression velocities.

- The windshield of the production Malibus broke early in these rollovers and, as shown in film of the vehicle's interior, the roof structure was deformed laterally back and forth several times as alternate sides of the roof struck the ground. This shows that the residual deformation of the roof of a rolled vehicle does not generally represent the maximum intrusion for a vehicle that has rolled more than once, nor does it indicate the maximum intrusion velocity.
- A stronger roof tends to reduce the trailing side loading forces.
- The front door side windows (tempered glass) of the production vehicles virtually all broke out leaving avenues of partial or complete ejection for a number of the unrestrained dummies.

- High head and neck loads are from rapid roof intrusion, not from the occupant diving into the roof.
- The circumstances of a rollover involving roof collapse have been documented by GM and Xprts, LLC photo-analyses and GM electronic instrumentation in the Malibu II test series. Table 1 consists of data from four production vehicles' roof to ground impacts in the Malibu II series where a restrained dummy suffered substantial neck loading.

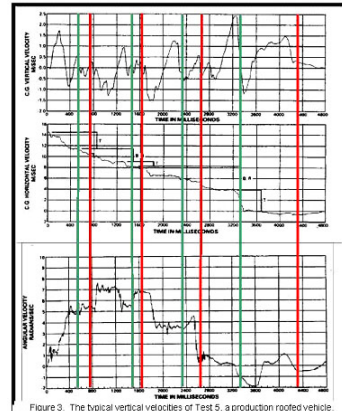


Figure 3. Contact Velocities in a Production Malibu.

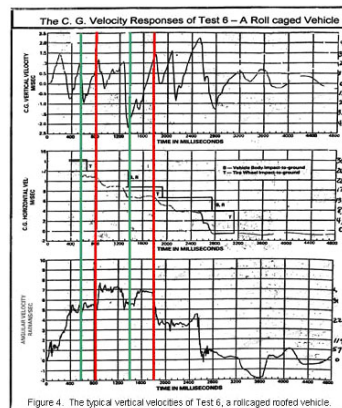


Figure 4. Contact Velocities in a Rollcaged Malibu.

- The typical vehicle roll angle of impact at the time of high roof rail intrusion velocity and injury measures was about 210 degrees. Another source of high intrusion velocity was roof panel buckling when the vehicle was at about 180 degrees.
- The typical vehicle roll angle of impact on the passenger side of these passenger side leading rolls was about 135 degrees.

GM Malibu I
Test 5
(All data from GM Discovery)
Near Side Contacts:
(Green Lines)
550 ms = 0.6 mph
1500 ms = 0.3 mph
2350 ms = 1.2 mph
3350 ms = 1.2 mph
Far Side Contacts:
(Red Lines)
790 ms = 0.6 mph
1677 ms = 0.4 mph
2662 ms = 1.2 mph
4330 ms = 0.7 mph

GM Malibu I
Test 6
(All data from GM Discovery)
Near Side Contacts:
(Green Lines)
575 ms = 2.2 mph
1500 ms = 2.5 mph
Far Side Contacts:
(Red Lines)
836 ms = 2.7 mph
1802 ms = 3.1 mph

- Based on unrestrained Hybrid III dummy drop tests a neck load of 7,000 N corresponds to a 2.4 m/sec (5.4 mph) impact/intrusion velocity while the average 3,867 N neck load of some 94 PIIs correspond to a 1.1 m/sec (2.4 mph) impact intrusion velocity.

In 1975, the lead engineer in these tests, Edward Moffatt, set forth the theory that occupant injury in rollovers was the result of diving into the roof rather than from the consequences of roof collapse or buckling. In this, he was supporting a position that General Motors had taken in the early 1970s when it opposed promulgation of a strong roof crush standard by the Federal government. The authors of the papers on the Malibu tests (who actually conducted the tests) claim that the Malibu tests demonstrated that high neck loads were a consequence of the occupant diving into the roof. However, the newly released test data clearly shows that the peak neck loads occurred significantly after onset of roof intrusion, and typically when the roof intrusion velocity was highest, as shown in Figure 5. Quotes and conclusions from the original paper will be referenced and discussed in view of the newly public information.

A REINTERPRETATION OF MALIBU I

The following quotations, from the Abstract of “Rollover Crash Tests – The Influence of Roof Strength on Injury Mechanics,” SAE 851734, October 1985, present General Motors’ views on how head and neck injuries are inflicted in rollovers. This paper reports on dolly rollover tests of four production and four roll caged 1983 Chevrolet Malibus. All of the front outboard seated dummies in these tests were unrestrained.

Table 1.
Characteristics of an automobile rollover illustrating the conditions during injurious impacts in Malibu II. Time lag is the time between roof touchdown to peak neck load and the speed is the traveling speed at touchdown.

PII	Neck Load (N)	Time Lag (ms)	Speed (mph)	Roll Angle at Neck Load	Vehicle Pitch at Neck Load
3L2	10,900	28	22.1 ±2.2	210°	5°
3L3	12,000	30	20.0 ±2.1	1+ 210°	7°
4L2	7,600	28	21.9 ±3.2	1 +225°	3°
7L4	13,200	5 + 12	6.7 ±.8	3 +190°	10°

Malibu 2, GM Analysis of “Potentially Injurious Impacts”

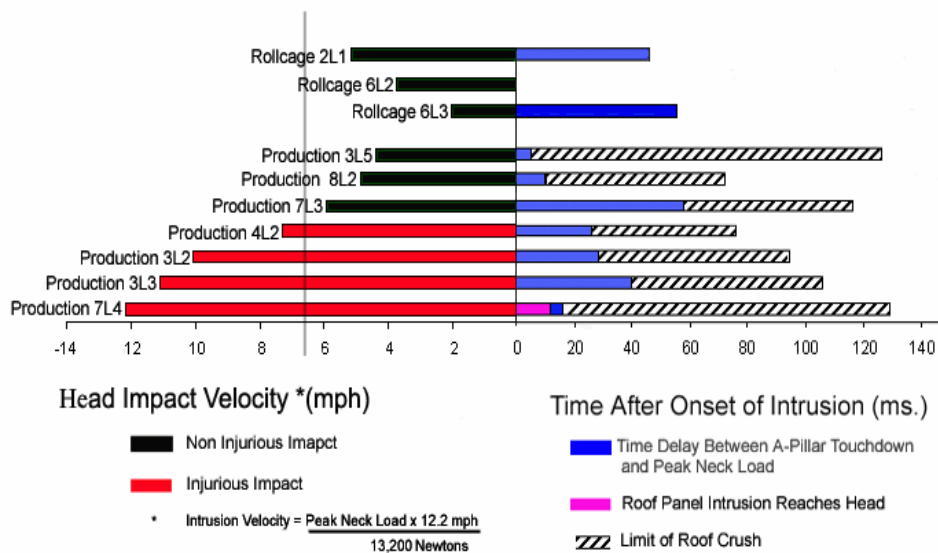


Figure 5. Head impact velocity and timing of GM selected impacts.

“... High head/neck loads were measured when the head contacted a part of the car experiencing a large change in velocity, often that part of the car which struck the ground.” (SAE 851734, p. 181)

“... The results of this work indicate that roof strength is not an important factor in the mechanics of head/neck injuries in rollover collisions for unrestrained occupants. ... There was no reduction in the incidence or severity of head/neck injuries in the roll caged cars compared with the standard roof vehicles. The roll caged vehicles incurred less glass breakage.” (SAE 851734, p. 181)

In these tests only two roof impacts resulted in a “large change in velocity” of the far side roof: impacts (1L3 and 4L4). Both were in production roof vehicles. Another head-to-ground impact accompanied by a “large change in velocity” (4L2) was to an ejected occupant (one of eleven partially or completely ejected occupants). None of these, out of a total of 54 measured impacts, occurred in vehicles with roll cages.

The other 51 dummy impacts had head or neck loads averaging less than half of these three and occurred at an average impact velocity of 2.6 mph. The three serious injury measures, in two of four production vehicle rollovers, are more than would be representative of the frequency of serious to fatal injuries in the U.S. vehicle population of the time as indicated by National Accident Sampling System (NASS) data.

Although not mentioned in the paper, GM recorded roof intrusion velocities of approximately 20 mph for 1L3 and approximately 3.1 m/sec (7 mph) for 4L4. The neck load from ground contact for 4R2 was also approximately 3.1 m/sec. As with the other 11 ejections, it was the result of side window breakage (18 out of 20 side and rear windows broke in production Malibus from ground contact while only 5 of 20 broke in roll caged cars).

The appropriate conclusion is that there were two high head/neck loads from a rapid roof intrusion on the trailing side and one high neck load from a near side partial ejection and ground contact in production vehicles while there were *none* in roll caged vehicles. The test engineers recorded a total of 50 other minor head impacts (none of which would have resulted in

serious injury). These head impacts included 10 other near side partial ejections; one total ejection and one head impact on the unpadded roll bar). Except for the ejections, these low injury potential impacts were about equally distributed among production and roll caged cars.

Dummy Head Impacts 1L3 and 4L4

In the same Malibu I paper, GM presented an explanation of two particular head impacts with high injury measures.

“In impacts 4L4 and 1L3 the left dummy head was against the roof panel in an area which struck the ground. ...It was not the displacement of the roof relative to the seat but, rather, the increased area of contact between the roof panel and the ground which defined this specific injury mechanism.” (SAE 851734, p. 193)

Figures 6 and 7 show a sequence of frames from the photographic documentation of 1L3 and 4L4 that demonstrate that the injury mechanism was, in fact, the roof displacement..

Figure 6 shows Malibu I Impact 1L3 in a sequence of interior views (at 4 ms timing per frame) of the driver dummy during roof intrusion of 12 inches at 20 mph velocity taking place over 32 ms. This roof intrusion produced a HIC of 2,820 to the dummy that is against the roof (from centrifugal force) and driven inward and towards the seat cushion. Notice the checkered seat back reference is stationary so that the path of the head can be followed by the sequence of yellow dots which locate the dummy's chin.

Figure 7 shows the Malibu I Impact 4L4 sequence of interior 4 ms frames of the driver being struck by a traveling buckle in the roof panel moving from the passenger side towards the driver side. The loading occurs in frame 6 when the neck is seen compressed and the dummy is subsequently driven towards the seat.

Shown below in Figures 8 and 9 are the vehicles at rest showing the extent of lateral roof crush to the vehicles in these tests.

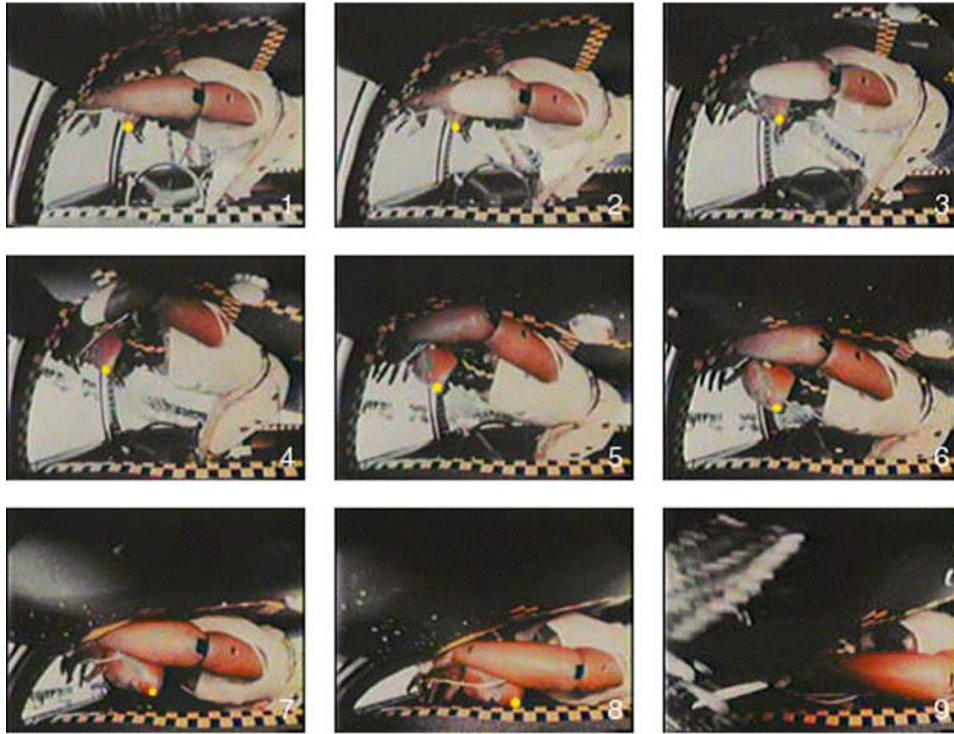


Figure 6. A sequence of frames from Malibu I, Impact 1L3.

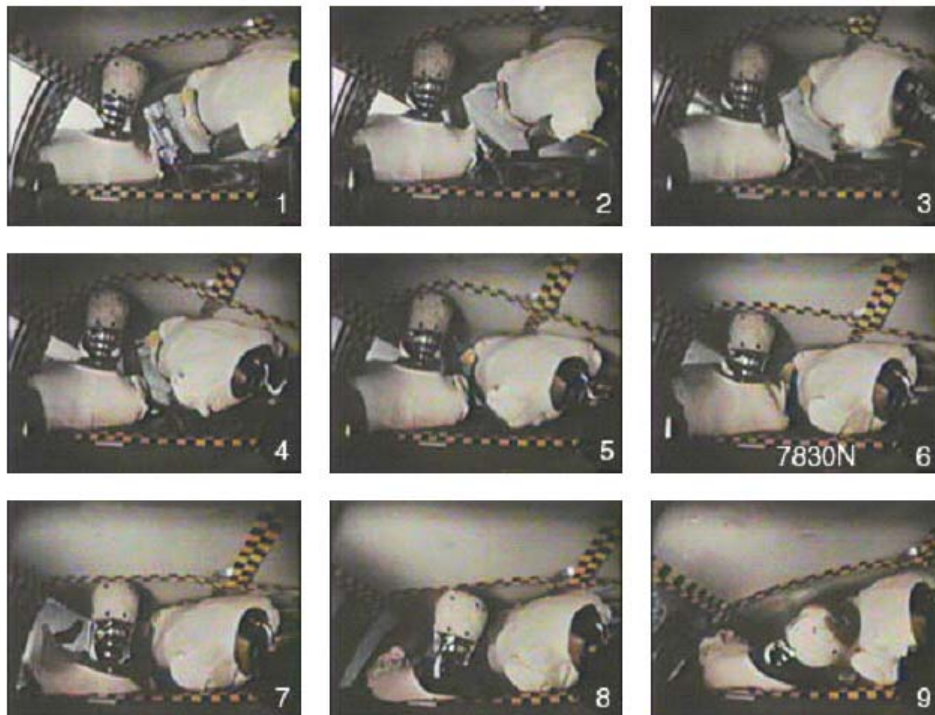


Figure 7. A sequence of frames from Malibu I Impact 4L4.

A REINTERPRETATION OF MALIBU II

The following quotations present General Motors' views on various aspects of occupant injury in rollovers. They are from "Rollover and Drop Tests-The Influence of Roof Strength on Injury Mechanics using Belted Dummies," SAE 902314, November 1990. This paper reports on dolly rollover tests conducted with four production and four rollcaged 1983 Chevrolet Malibus. All of the front outboard seated dummies in these tests were restrained by lap/shoulder belts that had cinching latch plates.

Neck Loads and the Neck Injury Criterion

The engineers who conducted the Malibu tests stated:

"In order to compare the injury mechanics in the roll caged vehicles with those of the standard roof vehicles, it was necessary to make a judgment as to which were the significant impacts to the head and neck." ... *The performance of the two types of vehicles were studied by comparing the number of "potentially injurious impacts" measured by the dummies.* (SAE 902314, p. 191, emphasis added)

GM states that the conclusions about injury should be based on injury potential, but theirs are not. Rather, GM elected to use an unrealistically low neck injury criterion of 2000 N. Such an impact would be produced by striking the head at only 2 mph (a very slow walking speed) which they said would produce "Potentially Injurious Impacts."



Figure 8. Malibu I Test 1 vehicle at rest with residual driver side intrusion.

The Advantage of a Strong Roof

The GM engineers concluded:

"The roll caged vehicles did not have any increased level of protection over the standard roof vehicles in these tests. The number of potentially injurious impacts for the roll caged vehicles was 28 compared to 26 for the standard roof vehicles. The average neck load measured in the roll caged vehicles was 3318 N compared with 3688 N in standard roof vehicles." (SAE 902314, p. 194)



Figure 9. Malibu I Test 4 vehicle at rest with residual front seat intrusion and tenting.

The following chart, Figure 10, of Malibu II shows that even using their reasoning, as the potentially injurious neck injury level is raised to 6,000 N the number of injuries was substantially lower in roll caged vehicles. This chart was generated by GM, but was not included in the paper.

BELTED ROLLOVER TESTS		
AXIAL NECK LOAD ANALYSIS		
	ROLLCAGE	PRODUCTION ROOF
Driver	4 r s @ 3663n	15 r s @ 5880n
Right Front	14 r s @ 3309n	7 r s @ 3643n
TOTAL	18 r s @ 3388n	22 r s @ 5168n
If cut off @ 3000	8 r s @ 4702n	16 r s @ 6156n
If cut off @ 4000	6 r s @ 5145n	14 r s @ 6500n
5000	3 r s @ 6000n	6 r s @ 9283n
6000	1 r s @ 6600n	5 r s @ 10,080n

Figure 10. GM's analysis of axial neck loads from the Malibu II test series.

The potential for injury comes not only from axial compression. When considering the trailing side occupant (the driver in the Malibu tests), the tables of Figure 11, show the substantially higher risk of injury from lateral bending moments, lateral shear forces, A-P Shear forces and A-P Moments in production as compared to rollcaged vehicles.

Kinematics of Rollovers

The GM engineers correctly observed that the passenger side of the roof contacted the ground first, followed by the driver side. They also observed:

“The difference in leading rail deformation between production and roll caged roofs resulted in the roll caged car rolling higher above the ground.” (SAE 902314, p. 105)

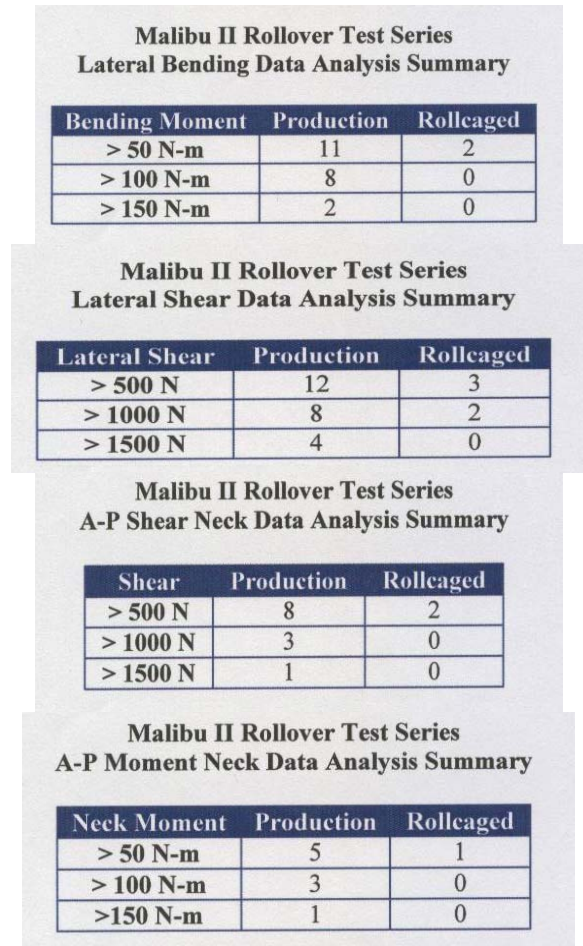


Figure 11. The numbers of impacts in which neck shear and bending moments exceed various limits in the Malibu II tests. (Reproduced from GM documents from the Malibu tests.)

“As its trailing rail approached the ground, this change in elevation, combined with the vehicle geometry, usually resulted in the trailing rail lightly striking or missing the ground in the roll caged car, whereas, for the production car, it usually struck the ground with greater severity. This slight change in elevation on the inverted vehicle resulted in a substantial increase in the velocity and

duration of the roof to ground impact of the trailing roof rail of the production vehicle as compared to the roll caged vehicle.” (SAE 902314, p. 105)

“In these tests, slight differences in the vehicle height above the ground resulted in major differences in the frequency and severity of the trailing roof rail impacts.” (SAE 902314, p. 105)

“This higher frequency and severity of neck loads to the driver dummy in production vehicles was the result of the increased number and severity of trailing rail-to-ground impacts as explained previously in the vehicle kinematics section.” (SAE 902314, p. 106)

We found it interesting that a secondary advantage of a strong roof – and one that perhaps should be considered when determining the benefits of strong roofs – is that it reduces the severity of ground impacts. However, a more important advantage of a stronger roof is that it reduces the frequency and severity of the trailing side roof impact loading, intrusion, intrusion velocity and therefore injury potential. In the FMVSS 216 test of the production Malibu, the average strength-to-weight ratio (SWR) of the trailing side as measured by our survey tool, was only 0.6:1 [5]. The roll caged Malibu had a SWR in excess of 7:1 in the FMVSS 216 test.

Figure 12 is a sequence of frames of the Malibu II Test 3 video showing the trailing side structure and driver dummy’s head and shoulders. It has been annotated with the sequential location of the intersection of the roof rail and B-pillar. The numbers 1, 3, 5, 7 and 8 show the roof after near side impacts while 2, 4, 6, and 9 show the roof after far side impacts. In this 3½ roll event, the trailing B-pillar rebounds elastically as well as from restoring forces from near side impacts. At position 8, just before the vehicle came to rest on its roof, the roof has virtually been restored to its original position. This behavior shows that residual roof crush, as used in statistical studies (without a detailed investigation of individual cases), can be misleading.

Comparisons between Production and Roll caged Roof Performance

The GM Engineers selected Malibu II impacts 3L5 (production) and 2L1 (rollcaged) for comparison. Specifically, they said:

“To analyze the effect of roof strength on neck loading, comparable driver dummy impacts were identified. The last one-half roll of test 2 (roll

caged) and test 3 (production) showed very similar roof-to-ground impacts, with the production car having significant roof crush. In the roll caged car which had no roof deformation, the driver dummy had an axial neck load of 5600 N. In the production roof vehicle, which had approximately 280 mm of roof crush, the driver dummy had an axial neck load of 4,700 N. In both instances the dummies were in very similar positions, the roof-to-ground impacts were of similar severity, with the ground impact velocities of 6.2 mph for the roll caged car and 6.8 mph for the production car. The neck loads were also similar despite the roof crush. Photo analysis of this impact reveals that the neck load measured by the dummy occurred when the roof hit the ground and the dummy head was on the inside of the roof panel.” (p. 106)

“The roof crush which is seen in the films is actually the vehicle body moving closer to the roof, which occurred after the peak force on the neck; consequently, this deformation had no effect on the severity of the head-to-roof impact. Figure 12 from Malibu paper (here shown as Figure 13) illustrates that the dummy neck loads occurred prior to vehicle roof crush.” (SAE 902314, p. 106)

“The PII’s with relatively higher neck loads in the production roof tests were studied using film analysis in conjunction with instrumentation data to determine when the loading was experienced by the dummy. This analysis confirmed that the peak load occurred at the roof to ground impact prior to the roof deformation.” (SAE 902314, p. 106)

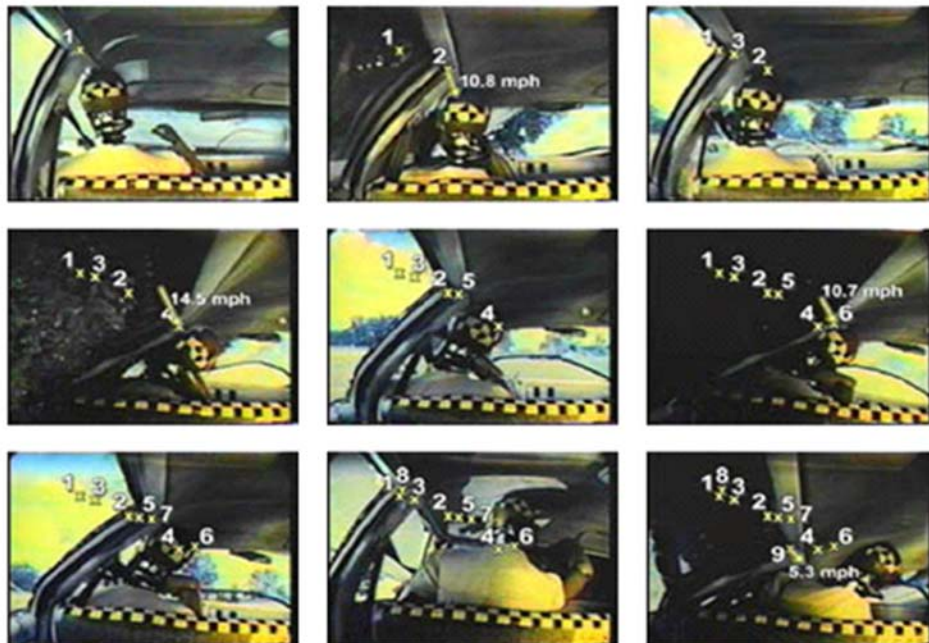


Figure 12. Malibu II Test 3 sequence of the intrusion position of the trailing side roof.

The pair 3L5 and 2L1 are not the only ones that can reasonably be compared. But GM’s photo analysis of the potentially injurious impacts (the first page of which is shown in Figure 14) and the summary charts of all analyzed impacts, Figure 15, show that the roof crush that produced the neck load occurred after a significant delay from the adjacent A-pillar ground contact: on average about 27 ms. after the roof began to crush.

To analyze the effect of roof strength on neck loading, many comparable driver dummy impacts were identified in addition to 3L5 v 2L1. Of the 10

analyzed by GM (See Figures 5 and 14) they include 3L3 v 6L1 and 7L4 v 2L1. GM deliberately chose a pair that had the same low neck load to suggest that there is no added protection from a strong roof vehicle.

The second roll of test 3 (3L3) and test 6 (6L1) showed very similar roof-to-ground impacts, but the production car suffered substantial roof crush from that roof impact. In the roll caged vehicle, which had no roof deformation, the driver dummy had an axial neck load of 2,800 N. In the production roof vehicle, which had 225 mm of roof crush, the driver dummy

had an axial neck load of 12,000 N. In both instances the dummies were in very similar positions, the roof-to-ground impacts were of similar severity. The neck loads however were vastly different because of the difference in roof intrusion velocity which was 6.3 m/sec (14 mph as determined from the initial slope of the roof crush versus time graph) for test 3 but only 2.2 m/sec for test 2; and roof crush which was 23 cm (9 inches) for test 3 but less than 3 cm for test 6 (see Figure 16, 17, and 18).

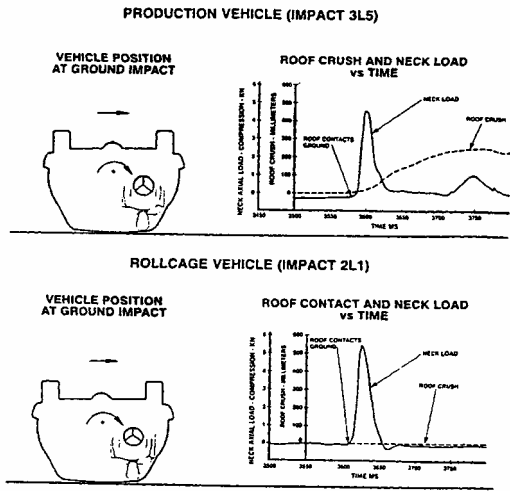


Figure 13. (Figure 12 in the Malibu II paper.) Roof Crush and Neck Loads versus Time from a GM Comparison between 3L5 (production) and 2L1 (roll caged).

Photo analysis of these impacts reveals that the production vehicle neck load measured by the dummy occurred approximately 26 ms after the roof hit the ground and the dummy head was on the inside of the roof panel. The first four inches of high speed roof crush intrusion, which is seen in the films, occurs before the peak force on the neck. The maximum (or residual) deformation had no effect on the severity of the head-to-roof impact. Figure 16 illustrates that the high dummy neck loads occurred after the initial four inches of high speed intrusion but before the maximum roof crush.

The last roll of test 7 (7L4) and test 2 (2L1) showed very similar roof-to-ground impacts, with the production car having substantial roof crush. In the roll caged vehicle, which had no roof deformation, the driver dummy had an axial neck load of 5,000 N (which would not produce serious injury). In the production roof vehicle, which had 225 mm (9 inches) of roof crush, the driver dummy had an axial

neck load of 13,200 N. In both instances the dummies were in very similar positions, the roof-to-ground impacts were of similar severity. The neck loads however were vastly different because of the difference in roof intrusion velocity which was 6.3 m/sec (from the buckle moving from right to left) for test 7, and 1.4 m/sec for test 2; and roof crush which was 23 cm for test 7, and 3 cm for test 2.

ANALYSIS OF POTENTIALLY INJURIOUS IMPACT 2L1

1. The view for film analysis was the front view. Vehicle yaw prevented use of side view. This is a Locam camera.
2. Frame rate by film analysis is:
243.2 frames/second or,
1/243.2 fr/sec = .00411 seconds/frame
3. Film analysis begins at frame 825. Time zero is the strobe flash inside the vehicle as it touches the end of the rail.
825 frames X .00411 sec/frame = 3391 milliseconds
4. Zero milliseconds on the film analysis plots, figures 2-2L1, 3-2L1 and 4-2L1, corresponds to 3391 ms.
5. In figure 1-2L1, peak neck axial compression occurred at 3630 ms.
6. The driver side A pillar just touches the ground at frame 872 or 3584 ms.

Figure 14. The first page of the 2L1 set of the 10 sets of photo analysis.

Test No.	Occ.	Impact #	A-pillar touchdown time	Time of peak neck load	Delay (ms)	Time of end of roof crush	Peak neck load (newtons)
2	L	1	3584	3630	46	---	5500
3	L	2	582	610	28	648	10900
3	L	3	1290	1330	40	1356	12000
3	L	5	3590	3595	5	3711	4400
4	L	2	1281	1307	26	1331	7600
6	L	2	2163	2163	0	2163	4200
6	L	3	3258	3313	55	---	2500
7	L	3	2538	2553	15	2596	6700
7	L	4	3782	3787	5	3906	13300
8	L	2	1552	1562	18	1614	5400

Figure 15. The summary chart of the 10 photo analysis showing that there is a significant delay between the beginning of crush (A-pillar touchdown) and peak neck load.

Photo analysis of these impacts reveals that the production vehicle neck load measured by the dummy occurred approximately 200 ms after the near side roof hit the ground and a roof panel buckling wave (what GM called a contact patch in Malibu I, but did not mention in Malibu II) struck the dummy's head which was pressed against the inside of the roof panel. The first four inches of high speed roof crush intrusion, which is seen in the films, occurs before the peak force on the neck; although the maximum (or residual) deformation had no effect on the severity of the head-to-roof impact. Figures 19, 20 and 21 illustrate that the high dummy neck loads

occurred after the initial four inches of high speed intrusion but before the maximum roof crush.

In the case of impact 7L4, the GM engineers opined:

“Figure 13. [Impact 7L4, shown as figure 22 here] ... First the load on the dummy neck is the result of the dummy head stopping against the roof when

the roof is against the ground. When the dummy head stops, the dummy torso continues to move toward the head, causing high axial forces in the neck. The neck measurements indicate that the peak of the force pulse occurred approximately 10 ms after the adjacent roof panel struck the ground, which was before any significant roof crush occurred.” (SAE 902314, p. 106)



Figure 16. A sequence of frames from Malibu II Impact 3L3.

Impact	3L3	6L1
Roll Angle	217°	225°
B-Pillar Displacement	16.7 in	0 in
Peak Neck Load	12,000 N	2,800 N
Vehicle Rotation Rate	407°/sec	500°/sec
B-Pillar Velocity	10.7 mph	0 mph

Figure 17. Comparison of Malibu II Impacts 3L3 (Production) and 6L1 (Roll caged).

We have redrawn their Figure 13 from the Malibu II paper as Figure 23 here to reflect detailed measurements of right and left B-pillar acceleration, the interior intrusion and intrusion velocity. With the

original film there is sufficient resolution to track the motion of the roof directly above the dummy’s head.

The load on the dummy neck is the result of the dummy head being contacted by the deformation of the roof panel from the near side ground contact and intrusion. That contact also forms a traveling buckle in the roof panel starting on the near side and traveling across the vehicle roof to merge with the trailing side contact and intrusion. The traveling buckle has an amplitude of about 4 inches and is off the ground and intrudes on the dummy head at 12 mph, causing the peak neck load over about 12 ms.

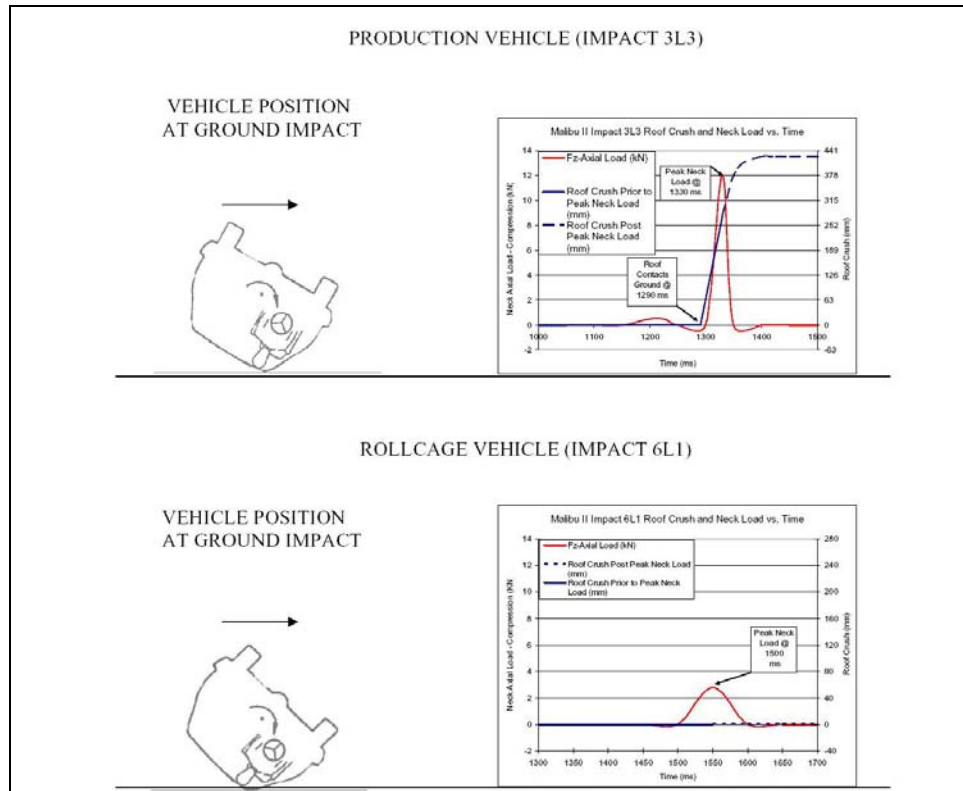


Figure 18. Roof Crush and Neck Loads v. Time for Impacts 3L3 (prod.) and 6L1 (roll caged).



Figure 19. Nine frames from impact 7L4 with timing referenced.

Impact	7L4	2L1
Roll Angles	176°	184°
B-Pillar Displacement	9.8 in	0 in
Peak Neck Load	13,200 N	5,600 N
Vehicle Rotation Rate	172°/sec	184°/sec
Vehicle Horizontal Velocity	6.7 mph	6.5 mph

Figure 20. Comparison of Malibu II Impacts 7L4 (Production) and 2L1 (Roll caged).

The GM engineers did not consider the pitched roof A-pillar being in contact with the ground and, as a consequence of the lateral compression of the roof panel, forming a traveling buckle that intrudes rapidly into the compartment. The continuation of the trailing side roof intrusion then drives the dummy toward the seat, after the neck injury. The traveling buckle is very much like the panel motion in Malibu I

4L4, that the GM authors called a “contact patch” as we explained earlier. Figure 24 depicts the sequence of sample frames shown in Figure 22, starting at the near side contact, then the three frames during which the buckle compresses the neck at an intrusion speed of 12.2 mph and the merging of the buckle with the far side roof crush driving the dummy towards the seat.

Drop Test Results – Vehicle Kinematics

As an additional part of the Malibu test series, the engineers dropped vehicles onto their roofs with standing pelvis (pedestrian) dummies restrained in them. They concluded, “The roll caged vehicles had no perceptible crush on impact.” (SAE 902314, p. 109) They added, “Overall, in these drop tests, roof crush did not appear to adversely affect the neck loads to the unbelted or belted dummies which were seated in the area of impact.

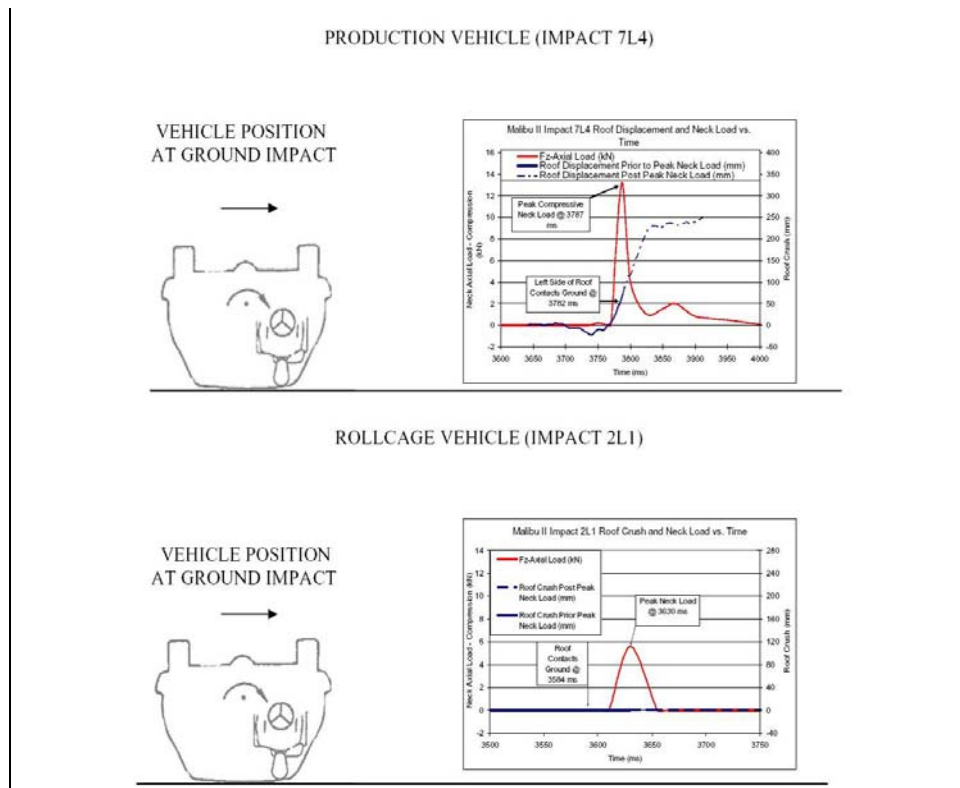


Figure 21. Roof Crush and Neck Loads v. Time for Impacts 7L4 (prod.) and 2L1 (roll caged). The roof displacement in 7L4 is measured over the driver dummy’s head.

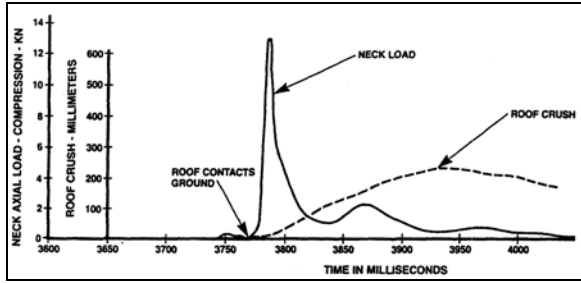


Figure 22. Figure 13 of the Malibu II paper.

Figure 25 from the roll caged drop test demonstrates that at touchdown, indicated by the flash, the roll caged vehicle drops two inches (as shown by the arrow) while deforming the crown of the roof at the dummy head contact point prior to the roll caged structure engaging the ground. As a result the production and roll caged vehicles performed identically (with the same dummy).

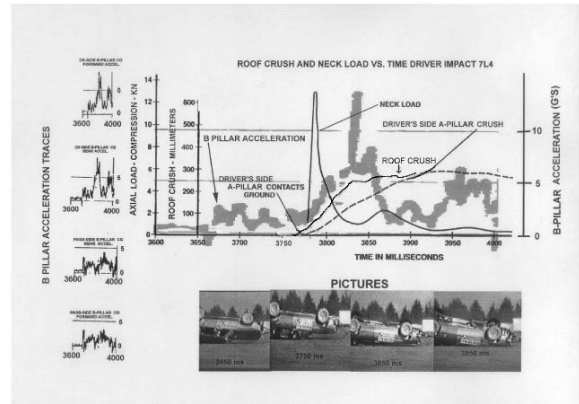


Figure 23. 7L4 redrawn to reflect the correct timing perspective and the timing of the B-pillar accelerometer traces.

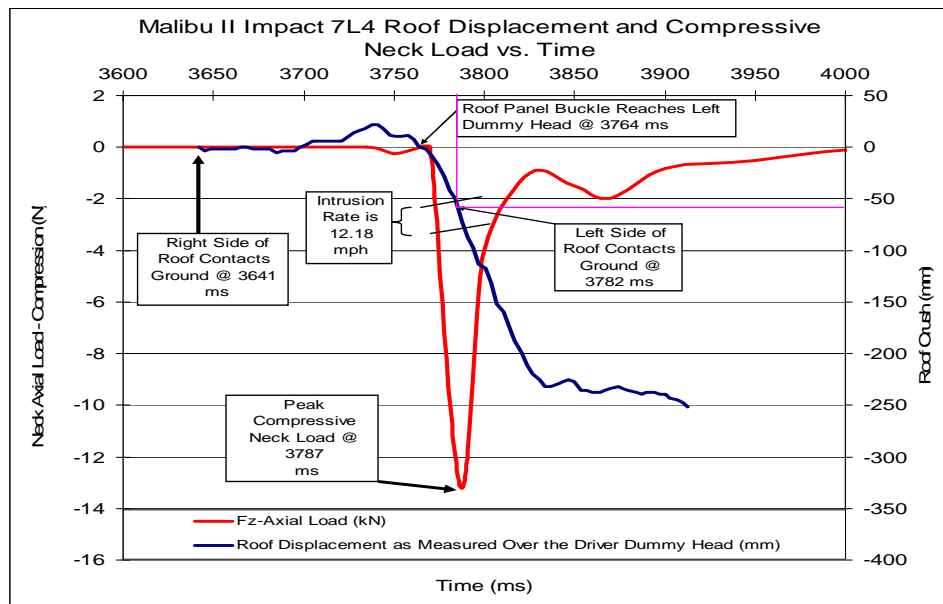


Figure 24. The motion of the roof above the driver dummy's head relative to a reference line.

Although not stated in the paper, the dummies used in these tests were standing, not seated pelvis dummies (with the probable exception of the belted driver in the production vehicle drop test). A subsequent test conducted by one of the authors with the same vehicle, with a production belted human and a seated pelvis dummy in a rigid roll caged vehicle showed a major difference in neck loading, Figures 26 and 27.

The Mechanism of Neck Injury

The Malibu II data show clearly that:

- During a rollover, the vehicle drop height is insufficient to cause a neck injury. The impact speed of the head with the vehicle roof when the roof does not collapse is less than a normal human walking speed.
- The mechanism of neck injury in rollovers is roof crush where the low falling speed of the occupant is substantially exacerbated by the rapid intrusion

of the collapsing roof to produce excessive neck loads.

- The results of Figure 10 show that even using their methodology, as the potentially injurious neck injury level is raised to 6,000 N, the number of potentially injurious impacts would be substantially lower in roll caged vehicles. In fact, if the cut off were raised to 7,000 N, a value that is shown by Hybrid III biomechanics research to be a threshold for dummy neck injury, there would have been no potentially injurious impacts in the roll caged vehicles.

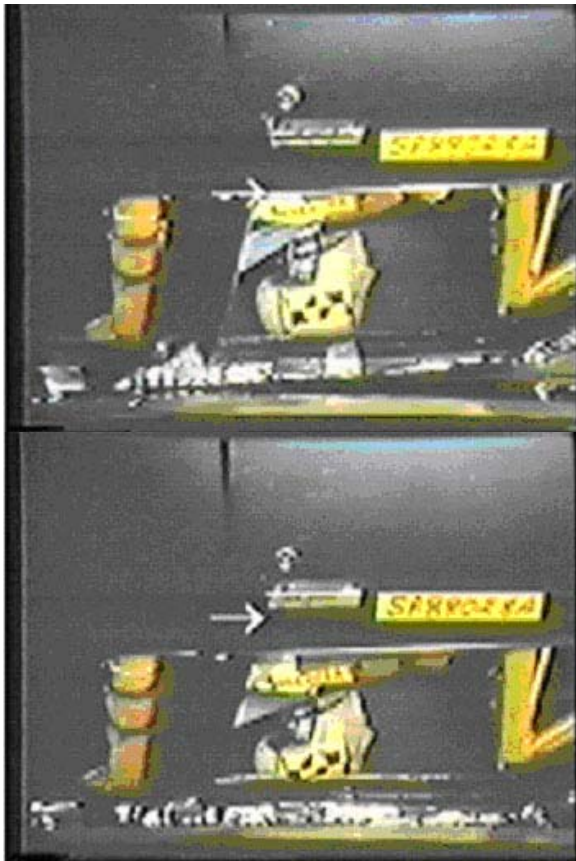


Figure 25. Sequence of photos from roll caged Malibu drop test.

Despite this evidence, the engineers who conducted these tests insisted that:

“Neck loads resulted from “diving” type impacts where the head stops and the torso momentum compresses the neck, with the magnitude proportional to the impact velocity” (SAE 902314, p. 111)

In both of the GM Malibu papers, the authors present a theory that the occupants have high neck

loads because they are diving into the ground as the vehicle rolls. In their view, the injury occurs when the roof comes into contact with the ground and the occupant’s head, which is in close proximity to the roof, also strikes the ground through the roof. As a consequence, the vertical motion of the occupant’s head is stopped. The claim is that at that point the occupant’s body is still moving downward and imposes an injurious force on the neck because the neck is compressed between the head and the body. This is similar to what happens to a person who dives into a shallow pool.



Figure 26. One of the authors (Friedman) and a Dummy in a 5.4 mph Malibu Drop Test in which roof crush was precluded.

	Production Belted Standing Pelvis Dummy	Production Belted Seated Pelvis Dummy	Production Belted Iliac Crest Pelvis Human
Lap Loop Load	2,136 N	5,106 N	8,432 N
Head Force Z	6,915 N	4,255 N	(not measured –lightly struck roof)
Total Force	9,051 N	9,361 N	> 8,432 N

Figure 27. A comparison of data from Seated vs. Standing Dummies and a human subject.

GM’s theory may at first glance seem reasonable, but at the time a strong roof strikes the ground, the motion of the occupant’s head (and body) is mostly horizontal. Thus, the speed with which the occupant’s head strikes the ground (through the roof) is about the same as the falling velocity of the CG (3 mph) and is insufficient to cause a diving type injury.

The Malibu Figures of 16 and 19, above, taken from the package shelf behind the rear seat offer no perspective of the fore and aft position of the dummy head. In reality the dummy neck is stiff compared to a human and gives the impression that the head does not bend. In rolling, with a Malibu cinching latch

plate belt a human person typically does not ‘dive’ into the roof (provided the rate of roll is sufficient) but is certainly not tightly in the seat at all times.



Figure 28. A human volunteer wearing a seat belt in the “Wonder Wheel”[6] that is rolling through 360 degrees. The occupant of this rotating fixture does not experience diving into the roof because his motion is essentially circular so that when the occupant’s head is nearest to the ground, it is traveling parallel to the ground.

We have illustrated this point with the “Wonder Wheel,” a device that simulates the motion of a rolling vehicle cab but with no roof crush or intrusion velocity. A human volunteer test subject is shown in Figure 28. His head moves to about the middle of the roof rail (even without vehicle pitch) and rises and

falls about 4 inches (in relation to the vehicle interior) during the rollover sequence.

CONCLUSION

The Malibu tests were well-designed and conducted, and provided a wealth of excellent data and film that has provided considerable insight into the mechanisms of occupant injury in rollovers. Furthermore, these tests show the value of a strong roof as a countermeasure to prevent severe head and neck injuries in rollovers.

It is unfortunate that the engineers who conducted these tests misinterpreted the results and that General Motors refused for two decades to release the raw data so that other scientists could review the validity of their interpretation. The consequences were that proper peer review of this work was impossible, and that the misinterpreted results were used to delay the provision of adequate rollover protection in new vehicles.

It is critical that other scientists conduct further review of this data to ensure that all scientists and engineers in the auto safety community understand and derive a consensus on the importance of strong roofs for rollover occupant protection.

REFERENCES

- [1] NHTSA Docket 1999-5572, (dms.dot.gov).
- [2] Bahling, G.S., Bundorf, R.T., Kaspzyk, G.S., Moffatt, E.A., Orłowski, K.F., and Stocke, J.E. “Rollover and Drop Tests – The Influence of Roof Strength on Injury Mechanics Using Belted Dummies.” *SAE 902314*, 1990. A more complete set of documents and films from this research has been placed in Docket NHTSA-1999-5572.
- [3] Orłowski, K.F., Bundorf, R.T., and Moffatt, E. A. “Rollover Crash Tests – The Influence of Roof Strength on Injury Mechanics.” *SAE 851734*, 1985
- [4] NHTSA Docket 1999-5572 (dms.dot.gov) CFIR Comment 10, April 2003.
- [5] Friedman, D. and Nash, C. E., 2003, “Measuring Rollover Roof Strength for Occupant Protection,” *IJCrash 2003*, Vol. 8, No. 1, pp 97 – 105.
- [6] Bish, J., Honikman, T., Sigel, J., Nash, C.E., and Friedman, D., “Human Response to Dynamic Rollover Conditions,” *ASME IMECE 2003*.